WILEY *Journal of* SURGICAL ONCOLOGY

A practical guide for the use of indocyanine green and methylene blue in fluorescence-guided abdominal surgery

Labrinus van Manen BSc[1] (ID) | Henricus J. M. Handgraaf MD, PhD[1] | Michele Diana MD, PhD[2,3,4] | Jouke Dijkstra PhD[5] | Takeaki Ishizawa MD, PhD[6] | Alexander L. Vahrmeijer MD, PhD[1] (ID) | Jan Sven David Mieog MD, PhD[1]

[1] Department of Surgery, Leiden University Medical Center, Leiden, The Netherlands

[2] IHU-Strasbourg, Institute of Image-Guided Surgery, Strasbourg, France

[3] IRCAD, Research Institute against Cancer of the Digestive System, Strasbourg, France

[4] Department of General, Digestive and Endocrine Surgery, University Hospital of Strasbourg, Strasbourg, France

[5] Division of Image Processing, Department of Radiology, Leiden University Medical Center, Leiden, The Netherlands

[6] Hepato-Biliary-Pancreatic Surgery Division, Department of Surgery, Graduate School of Medicine, University of Tokyo, Tokyo, Japan

Correspondence
Jan Sven David Mieog, MD, PhD, Department of Surgery, Leiden University Medical Center, Albinusdreef 2, 2300 RC Leiden, The Netherlands
Email: j.s.d.mieog@lumc.nl

Near-infrared (NIR) fluorescence imaging is gaining clinical acceptance over the last years and has been used for detection of lymph nodes, several tumor types, vital structures and tissue perfusion. This review focuses on NIR fluorescence imaging with indocyanine green and methylene blue for different clinical applications in abdominal surgery with an emphasis on oncology, based on a systematic literature search. Furthermore, practical information on doses, injection times, and intra-operative use are provided.

KEYWORDS
image-guided surgery, near-infrared, oncology, optical imaging, tumor

1 | INTRODUCTION

Cancer is one of the leading causes of death worldwide, resulting in 8.2 million deaths annually.[1] Treatments for cancer include surgery, radiation therapy, chemotherapy, and targeted therapies. Surgery is often the cornerstone in the treatment of solid cancers in the abdominal cavity. Especially during oncologic surgery, it is pivotal to remove as much tumor as possible and simultaneously to prevent unnecessary damage to surrounding healthy tissue. Despite that the quality of preoperative imaging modalities, such as MRI and CT, has been improved during the last decades, intraoperative navigation using CT or MRI is only performed in specialized hospitals, mostly confined to the field of neurosurgery, due to the complexity, high

costs, tissue deformation, and long acquisition times.[2] Today, for intraoperative navigation, the surgeon has to rely in the majority of the cases only on visual and tactile feedback to distinguish between different kind of tissue structures. Additionally, (laparoscopic) intraoperative ultrasound or sometimes a gamma probe can be used during oncologic surgery. However, this is not always sufficient. Tumor-positive (R1 or R2) resection margins in colorectal cancer, for example, occur in approximately 10% of the operated patients.[3,4] Together with the increasing rate of minimal invasive (laparoscopic and robotic) surgery and therefore the lack of tactile feedback, there is a demand of improving visibility of different kind of tissue types, especially for distinguishing malignant and benign structures.

In the past years, new intraoperative imaging systems that exploit the near-infrared (NIR) light spectrum, have been evaluated (pre) clinically for different applications.[5–8] For intraoperative purposes, NIR light (700-900 nm) is more advantageous than visible light due to its capability to penetrate deeper into tissue, up to 10 mm. In addition, in the NIR spectrum tissue exhibits almost no autofluorescence. NIR fluorescent contrast agents lead therefore to maximized signal-to-background ratios and enhance the contrast of different tissue types.[9,10] NIR fluorescence imaging requires a NIR fluorescent agent (ie, fluorophore) combined with an imaging system that is able to both excite and detect the fluorophore. The fluorescence signal can be visualized after milliseconds, which is advantageous above other emerging imaging techniques, such as Raman spectroscopy or Optical Coherence Tomography, which require more time to visualize the same field of view.[11] Moreover, most systems are capable of merging fluorescence signals with normal RGB color videos, allowing direct anatomical orientation.

Different fluorophores have been evaluated (pre)clinically in NIR fluorescence imaging. These fluorophores have to be injected locally or systematically before surgery. Today, only two of them, indocyanine green (ICG) and methylene blue (MB), are approved for clinical use by the Food and Drug Administration and the European Medicines Agency. 5-aminolevulinic acid (5-ALA) is also clinically used as a fluorophore, especially in the field of neurosurgery field. However, this dye is fluorescent at 510 nm, which is outside the NIR spectrum.[12] Consequently, the penetration capacity of 5-ALA is negligible. ICG and MB are nonspecific contrast agents in the near-infrared region and they do not bind to tumor ligands. ICG has a half-time of 150–180 s and is solely cleared by the liver.[13] Its excitation peaks around 800 nm. ICG is very safe; adverse events are reported in less than 1 in 40 000 patients and mostly comprise hypersensitivity reactions.[14] MB in low doses (<2 mg/kg) is safe, however it can induce severe adverse effects such as arrhythmias, coronary vasoconstriction, and hemolytic anemia in patients with renal insufficiency or after administration of higher doses.[15] MB is partially renal cleared and has an excitation peak of approximately 700 nm. Therefore it has a less tissue penetration capacity and background tissue shows more autofluorescence. Due to their differences in clearance patterns ICG and MB have been used for various applications. In short, the indications can be used for lymph node mapping, detection of vital structures (eg, ureters, bile ducts), identification of tumors, and assessment of tissue perfusion. This review provides a practical approach for NIR fluorescence imaging with ICG and MB for different clinical applications in abdominal surgery, with an emphasis on oncology.

2 | METHODS

We searched in PubMed for in human (in vivo) trials using ICG and MB in NIR fluorescence guided abdominal surgery, published before January 2018. The search was based on the following search items: "Indocyanine green" or "ICG," "Methylene Blue" or "MB,"

"Near-infrared" or "NIR," and "Fluorescence" or "fluorescent." More specific search terms were added per application (SLN mapping, tumor detection, tissue perfusion, detection of vital structures). Only articles written in English were included. Case reports and (systematic) reviews were excluded from the analysis. After selection of relevant articles, clinically relevant information focussing on how to perform NIR fluorescence imaging in daily practice was extracted from the articles to set-up a review. In this article, the different applications of NIR fluorescence in abdominal surgery, SLN mapping, tumor detection, visualization of vital structures and tissue perfusion, are discussed separately.

3 | RESULTS

Our search revealed a total of 891 articles, which are reported in a flow diagram (Figure 1). After exclusion of 720 articles, who did not meet our eligibility criteria, a total of 171 original articles remained, which formed the basis of this review.

4 | SENTINEL LYMPH NODE MAPPING

Sentinel lymph node mapping is only part of standard care in melanoma and breast cancer.[16,17] Current standard-of-care is a combination of blue dye and gamma probe for Technetium-99m (Tc-99m) detection, which has certain disadvantages. Blue dye has no penetration capacity whatsoever and a gamma probe does not allow visual identification. SLN mapping is not part of standard clinical care in abdominal oncological surgery.[18,19] Today, NIR fluorescence imaging of SLN(s) as a new and additional modality was evaluated for SLN mapping in malignancies of the oesophagus, stomach, colon, bladder, prostate, cervix, endometrium, and ovarium.

4.1 | Clinical applications

4.1.1 | Esophageal cancer

Esophageal cancer is a disease with a dismal prognosis, showing an overall 5-year survival rate around 14%.[20] Extensive lymphadenectomy improves the prognosis, especially at early stages.[21–23] To visualize the sentinel lymph nodes, ICG was evaluated as a NIR fluorescent marker in three clinical studies. All studies were feasibility studies and therefore using a small study population: 1-20 patients.[24–26] Ninety-five percent of the sentinel lymph nodes could be detected in the cohort of 20 patients, as shown by Yuasa et al.[25] However, further research is necessary before introduction into clinical practice.

4.1.2 | Gastric cancer

Gastric cancer is one of the most common cancers in the world, especially in Eastern Asia with an incidence of 24 and 9.8 per 100 000 in men and women, respectively. We found ten clinical studies using
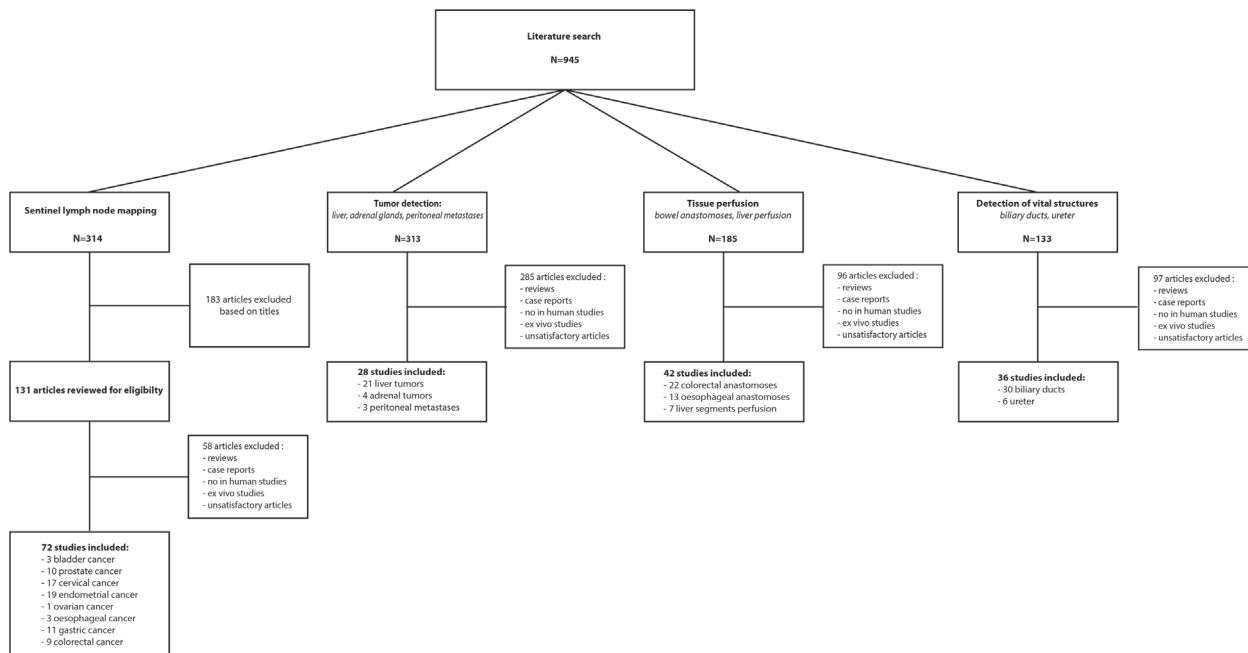
FIGURE 1 Flow-chart of the literature search strategy

ICG during NIR fluorescence imaging during laparoscopic or open gastric surgery.[27–36] The SLN identification rates ranges from 90% to 100%, however it decreases to 0% for T4 tumors.[35] It also has to be mentioned that most studies did not include these higher stages in their study, which could explain the high resection rates. In Japan and Korea, T1N0M0 tumors are standard treated with endoscopic resection, which creates new opportunities for clinical use of NIRF for SLN mapping in selected cases, as demonstrated by Bok et al.,[37] who showed that a combination of endoscopic submucosal dissection and sentinel node navigation surgery (laparoscopic) was feasible in 12 out of 13 patients.

4.1.3 | Colorectal cancer

SLN mapping in colorectal cancer is still a controversial procedure, due to the relatively low visibility of the lymphatic system after injection of blue dye.[38] In the past years NIR fluorescent imaging with other available dyes, such as ICG, was used in nine clinical studies during surgery.[29,39–46] All studies were performed in a small population, ranges from 5 to 30 patients, who underwent laparoscopic or open surgery due to colorectal cancer. The SLN detection rates by NIR fluorescence imaging vary between 65.5% and 100%, which could probably explained by the experience in the participating centers.

4.1.4 | Bladder cancer

A cystectomy with pelvic lymphadenectomy is the treatment of choice for patients with bladder cancer. However, accurate intraoperative detection of SLNs is difficult and lacks sensitivity.[47] Moreover, there is a great inter-patient variability in lymph drainage patterns, which makes the location of the SLN unpredictable. Recently, NIR

fluorescence imaging using ICG could detect a sentinel lymph node in at least 90%, which indicated that this technique could contribute to improved intraoperative staging of bladder cancer.[48–50]

4.1.5 | Prostate cancer

Prostate cancer is one of the most common cancers in men and treatment consists of diverse interventions, including surgical resection.[51] (Extended) lymph node dissection is sometimes performed during radical prostatectomy, depending on the preoperative risk assessment.[52,53] Ten studies evaluated the use of ICG during prostatectomy, which showed a high detection rate of SLNs, however due to the low prevalence of SLN metastases a low positive predictive value was found.[54–64] This supports the findings that NIR fluorescence imaging could be useful in high risk groups.

4.1.6 | Cervical cancer

Early stage cervical cancer, which is often detected by screening, is normally treated with radical hysterectomy and pelvic lymph node dissection.[65] Lymph node status is one of the independent prognostic factors for the patient's survival.[66] However, if the resected lymph nodes were not involved, which is often the case in early stage cervical cancer, patients underwent unnecessarily lymphadenectomy. This could be prevented by performing SLN mapping, for instance with NIR fluorescence imaging, as shown in different studies.[67–83] These studies, performed in early stage cervical cancer, showed detection rates varying from 60% to 100%. Recently, three studies compared ICG to the current golden standard for SLN mapping, blue dye and Tc-99m, in study populations varying from 58 to 144 patients.[73,74,76] It was concluded, that detection rates did not differ significantly

between blue dye with Tc-99m and ICG. However, all studies showed significantly higher rates of bilateral lymph node detection, especially in larger tumor sizes (>2 cm). Hence, it indicates that intraoperative lymph node mapping with fluorescence imaging using ICG is at least comparable to the current golden standard.

4.1.7 | Endometrial cancer

Endometrial cancer is one of the most common cancers in women and patients often presents with an early stage disease.[51,84] Currently, there is no agreement about performing SLN mapping to avoid extensive lymphadenectomy during surgery in early stage endometrial cancer.[19] However, in some centers fluorescence imaging is used for SLN mapping and incorporated in standard care.[85] Nineteen studies showed that fluorescence imaging is useful, indicating high detection rates of lymph nodes, varying from 68 to 100%.[69,71–73,78,80,83,86–97] Laios et al[69] showed the lowest detection rate (68%), which was probably caused by the learning process as visualized by a learning curve. Rossi et al[87] showed that cervical stromal injection of ICG is preferable over hysteroscopic endometrial injection for SLN detection, as illustrated by the significant difference in detection rates (82% vs 33% respectively, $P = 0.027$).[87] These results indicate that SLN mapping with NIR fluorescence imaging is feasible and may be worth considering for use in clinical practice.

4.1.8 | Ovarian cancer

One study evaluated the implementation of NIR fluorescence imaging of SLNs during laparoscopic surgery in seven patients with early-stage ovarian cancer.[98] In all patients, at least one SLN was detected after intraoperatively injection with ICG in both sides of the proper ovarian and suspensory ligament. Nevertheless, more studies have to be performed to determine the added value of fluorescence imaging for intraoperative lymph node staging, which is essential before implementation into clinical practice.

4.2 | Summary of findings

Sentinel lymph node mapping using ICG has been evaluated for several applications in abdominal surgery (gastroenterology, urology, and gynecology) with different imaging systems.[24–36,39–46,48–50,54–64,67–83,86–98] In these studies a high diversity in doses has been used, varying from 100 µg to 25 mg. In general, based on the evaluated clinical studies a dose of (at least) 2.5 mg is recommended for good visualization of sentinel lymph nodes.

It was shown, that ICG bound to human serum albumin (ICG:HSA) could also be used for SLN mapping.[26,79] Moreover, Hachey et al[26] showed that ICG:HSA is preferable above using ICG alone in esophageal cancer, which could probably be explained by the rapid lymphatic clearance and poor retention of ICG alone. However, due to the limited evidence we prefer an injection of ICG alone. As part of standard care, which consists of peritumoral blue dye injection, ICG could also be injected around the tumor. Most of the studies used a four quadrant

injection in the submucosa around the tumor. The timing of the injection is also an important issue. One study in gastric cancer prefers injection (endoscopically) 1 day before surgery.[36] They showed lower false negative results than intraoperatively subserosal injection, probably because of frequent leakage from damaged lymphatic vessels, caused by mobilising the stomach. On the other hand, most studies showed good results by performing injection, just after applying general anesthesia.[25,29,31,33,41,46,48–50,54,57,68–74,76,78,80,81,83,87–89,92,93,95,96]

For good visibility of the tumor and consequently a good injection place, a minimal-invasive (endoscopic, cystoscopic) approach is recommended, which also prevents damaging of lymphatic vessels. For cervical and endometrial cancer a cervical stromal injection of ICG is preferable above a hysteroscopic injection.[87] As shown in Figure 2, approximately 15–30 min after injection, the sentinel lymph nodes will be visualized.[33,39,43,50,62,89] In the mean-time the surgical procedure can be started, and the surgeon will therefore lose minimal time. After identification of the SLN(s) the additional oncological resection can be performed.

4.3 | How to use it

Taken together, optimal use of ICG for SLN mapping could be achieved by peritumorally injection of 2.5 mg ICG. Intraoperative injection, just after applying anesthesia, in a minimal invasive manner seems optimal. The SLNs could be visualized 15–30 min after injection (Table 1).

5 | TUMOR IMAGING

ICG has been used as a contrast agent for intraoperative detection of diverse tumor types, which is based on two characteristics of ICG: hepatic clearance and the enhanced permeability and retention (EPR) effect. Solid tumors (other than hepatobiliary tract) could be visualized by the EPR effect, which is based on the visualization with ICG of the increased permeability and reduced drainage in tumor tissue after tumor-induced angiogenesis.[99,100]

5.1 | Clinical applications

5.1.1 | Liver tumors (primary & secondary)

Due to its hepatic clearance, ICG can be used for imaging of hepatobiliary tumors, both metastases and primary liver cancers (cholangiocarcinoma and hepatocellular carcinoma). Healthy liver tissue clears ICG within a couple of hours, whereas tumor tissue retains ICG by compression of bile ducts. However, recent studies suggested also a molecular mechanism.[101,102] Immature hepatocytes, which are located in the transition zone between the tumor and normal liver parenchyma, were not able to excrete ICG into the biliary ducts due to down-regulation of anion transporters. This results in a fluorescent rim around the tumor or metastasis, making it easy to identify them. Furthermore, ICG accumulates into well-differentiated hepatocellular carcinoma (HCC), resulting in complete fluorescence
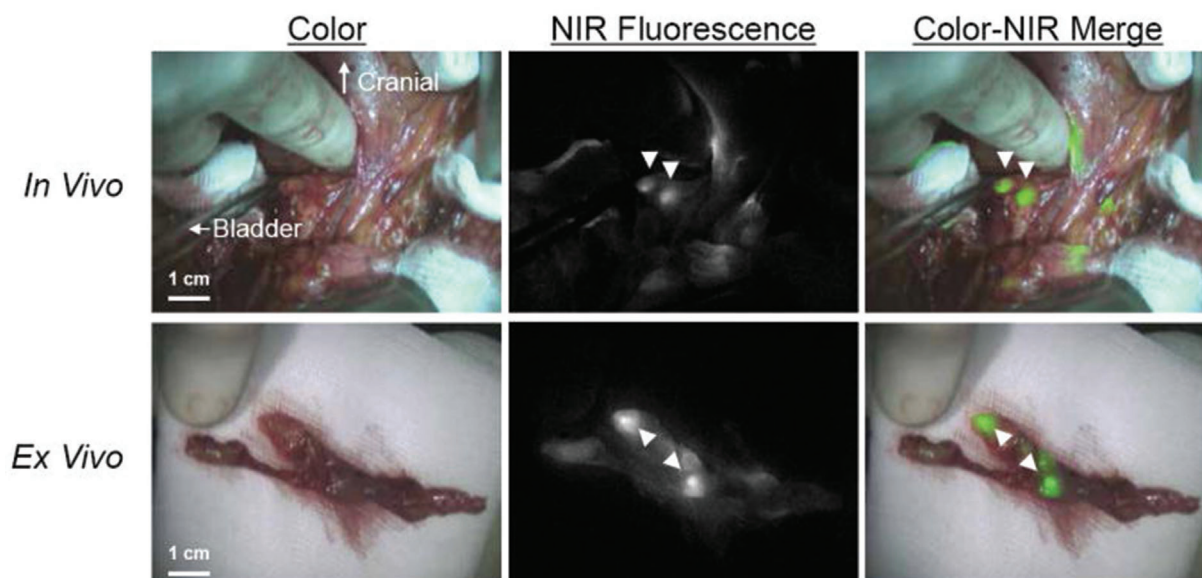
FIGURE 2 Example of lymph node mapping in bladder cancer during surgery and ex vivo. Upper panel: arrowheads indicate the NIR fluorescent lymph nodes along the left external iliac vein during surgery. Lower panel: fluorescent lymph nodes after excision. Reprinted by permission from John Wiley and Sons: Journal of Surgical Oncology[49] © 2014

signal rather than a dark center. In a retrospective cohort study in our institute it was shown that NIR fluorescence imaging of colorectal liver metastases was able to identify more and smaller tumors, resulting in reduced recurrences in a subset of patients.[103] Twenty-one studies evaluated the use of NIR fluorescence imaging with ICG for liver tumor detection, both primary tumors as metastatic spread of colorectal, uveal, breast, and pancreatic cancer.[101,102,104–122]

Summary of findings

To establish the optimal dose and injection time our group performed a comparison study with 10 and 20 mg ICG injection. However, no significant difference in optimal tumor-to-background contrast between respectively a 24 or 48 h administration and 10 or 20 mg injection was found.[122] Therefore, we recommend a bolus of 10 mg of injected intravenously 24 h before surgery based on clinical and logistical preferences. Tumor tissue compresses small bile ducts and consequently causes local inflammation. In these bile ducts and inflamed liver tissue ICG is retained for some days. Therefore, other groups showed also good results with ICG injection up to 14 days before surgery, although using much higher doses of ICG, up to 0.5 mg/kg.[101,106,108,109,111–113,117–120] Today, no randomized trial has been performed to compare these high differences in dosing and injection timing. After administering ICG, a fluorescent rim can be identified around tumors during surgery, as illustrated in Figure 3. Several studies showed that this technique not only identifies known tumors, but also occult, otherwise undetectable submillimeter tumors. However, only subcapsular lesions up to around 1 cm from the liver surface are expected to be visible, due to the limited penetration depth of NIR fluorescence.[123] Nevertheless, it could therefore be used as a complementary intraoperative tool, as

CT/MRI and intraoperative ultrasound still showed relatively high rates of false negatives for superficially located (subcapsular) lesions.[124,125]

5.1.2 | Peritoneal metastases

Preoperative detection of peritoneal metastases is often difficult with the current image modalities.[126] Adequate pre- and intra-operative staging is therefore an important issue for offering the best treatment. In the last years, more evidence is coming up, which showed that hyperthermic intraperitoneal chemotherapy (HIPEC) combined with cytoreductive surgery gave a better survival in patients with limited peritoneal metastases from colorectal or ovarian cancer.[127,128] Four (pilot) studies evaluated the intraoperative visibility of peritoneal spread in liver, colorectal, and ovarian cancer with NIR fluorescence imaging.[129–132] All studies showed a good visibility of peritoneal metastases, however in patients with ovarian cancer treated with HIPEC, distinguishing benign scars and malignant lesions was difficult.[131] Moreover, Tummers et al[132] showed a high false positive rate, which could be explained by the EPR effect, which underscores the need for tumor-selective targets. As HCC tissues often retain bile juice productivity even in metastatic sites, fluorescence imaging following preoperative intravenous injection of ICG can also be applied to identification of extrahepatic metastases of HCC.[130]

Summary of findings

All studies started with ICG injection 24 h before surgery. Unfortunately, no fluorescence signal was visible during exploration. However, intraoperative injection was feasible and showed good results. Hence, we recommend intravenously injection of ICG after abdominal

TABLE 1 Summary of known clinical applications of near-infrared fluorescence imaging in abdominal surgery and recommendations for intraoperative use

Application	Tissue type	Imaging system used in different studies	Preferred contrast agent	Recommended dose (mg)	Preferred injection site	Timing of injection	Time to visualize structures (min)
SLN mapping							
	Esophagus	Laparoscopic	Indocyanine green	2.5	Endoscopic: 4 quadrants injection	Just before surgery	15-30
	Gastric	Laparoscopic, open	Indocyanine green	2.5	Endoscopic: 4 quadrants injection	Just before surgery	15-30
	Colorectal	Laparoscopic, open	Indocyanine green	2.5	Subserosal: 4 quadrants injection	Intraoperatively	15-30
	Bladder	Robotic, open	Indocyanine green	2.5	Cystoscopic: bladder mucosa	Intraoperatively	15-30
	Prostate	Robotic, laparoscopic	Indocyanine green	2.5	Transrectal: under US guidance into prostate lobes	Intraoperatively	15-30
	Cervix	Laparoscopic, robotic	Indocyanine green	2.5	Transvaginal: submucosa cervix 4 quadrants injection	Intraoperatively	15-30
	Endometrium	Laparoscopic, robotic	Indocyanine green	2.5	Transvaginal: submucosa cervix 4 quadrants injection	Intraoperatively	15-30
	Ovarium	Laparoscopic	Indocyanine green	2.5	Laparoscopic: dorsal and ventral side of proper ovarian and the suspensory ligament	Intraoperatively	15-30
Tumor imaging							
	Liver	Open, laparoscopic	Indocyanine green	10	Intravenously	24 h before surgery	Directly
	Adrenal	Laparoscopic, robotic	Indocyanine green	2.5	Intravenously	Intraoperatively	1
	Peritoneal metastases	Open	Indocyanine green	0.25 (mg/kg)	Intravenously	Intraoperatively	>5
Vital structures							
	Bile duct	Laparoscopic	Indocyanine green	5	Intravenously	3-7 h before surgery	Directly
					Into gallbladder	Intraoperatively	Directly
	Ureter	Open, laparoscopic, robotic	Methylene blue	0.25 (mg/kg)	Intravenously	Intraoperatively	>10
Perfusion							
	Esophagogastric anastomoses	Laparoscopic, robotic	Indocyanine green	2.5	Intravenously	After mobilization and selecting of anastomotic site	1
	Colorectal anastomoses	Open, laparoscopic, robotic	Indocyanine green	2.5	Intravenously	After mobilization and selecting of anastomotic site	1
	Liver segments	Open	Indocyanine green	2.5	Portal vein	During surgery	2
		Laparoscopic	Indocyanine green	2.5	Intravenously	During surgery	2

exposition. A dose of 0.25 mg/kg of ICG could therefore be used. As shown above, detection of peritoneal metastases could be useful during intraoperative staging and cytoreductive surgery (combined with HIPEC). Clinical application of NIRF imaging during cytoreductive surgery should be reserved for patients with limited peritoneal spread (peritoneal cancer index <8).[129,133] If advanced peritoneal spread has been established preoperatively, the added value of fluorescence imaging with ICG is limited. After injection of ICG, peritoneal nodules become fluorescent from at least 5 min.[129] Tumor positive nodules become hyperfluorescent. Due to physiological accumulation of ICG,
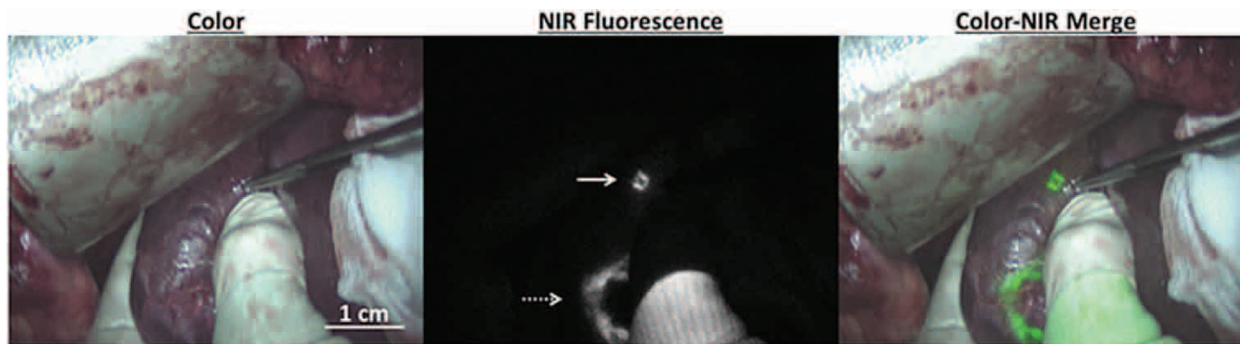
FIGURE 3 Example of two colorectal liver metastases detected by NIRF imaging. White arrow: a fluorescent lesion, which was not detected by preoperative imaging. Dashed arrow: a preoperative suspected lesion could be recognised by its characterizing fluorescent rim. Reprinted by permission from Elsevier: European Journal of Surgical Oncology[103] © 2017

detection of small peritoneal metastases is hampered in some abdominal regions (such as in the liver and visceral peritoneum).

5.1.3 | Adrenal tumors

Adrenal masses are often resected by performing minimal invasive surgery (laparoscopic or robotic).[134,135] Identification of the adrenal glands and determining the resection margins could be difficult, especially when it is surrounded by retroperitoneal fat. The added value of NIR fluorescence imaging using ICG during minimal invasive (partial) adrenalectomy has been determined in four studies.[136–139] Based on the difference in perfusion between the adrenals and the surrounding tissues, the adrenal glands and different types of adrenal tumors could be detected. Colvin et al[139] showed that NIR fluorescence imaging was superior and equivalent in 46.5% and 25.6% respectively, to conventional robotic view in determining the borders of the adrenal glands in 40 patients. Other mentioned studies showed similar results in determining the adrenal gland borders, however they were performed in much smaller populations.

Summary of findings

Three out of four studies used a 5 mg dose of ICG, which turned out to be the optimal dose for visibility of the adrenal glands.[136,138,139] After exposure of the retroperitoneum and acquiring a good view on the adrenal glands and its surrounding tissue, ICG could be intravenously injected. One minute after injection of ICG, the fluorescence signal could be detected.[139] First of all, the arterial vasculature of the adrenal glands and kidneys became fluorescent. After a few seconds, the fluorescence signal highlights the adrenal parenchyma, however it is slightly less fluorescent as the adjacent kidneys.[138] Adrenocortical tumors could be easily recognized by the hyperfluorescent signal, although medullary tumors (such as pheochromocytomas) were hypofluorescent during NIRF imaging.[138,139] In the background, the liver could show more intense fluorescence, in case of right adrenal surgery. The optimal tumor-to-background contrast is achieved after 5 min.[139] If the fluorescent signal washes out (>20 min after injection), a new injection of 5 mg ICG could be administered.

5.1.4 | Other solid tumors

ICG has also been evaluated in other solid tumors in the abdominal region, although the added value has not been proven. Our group studied the role of ICG for intraoperative visualization of pancreatic tumors during pancreaticoduodenectomy in eight patients.[140] After injection of ICG, only in one patients a clear tumor-to-pancreas contrast was observed. The use NIR fluorescence imaging during nephrectomy has also been a topic of research, as reviewed by Bjurlin et al.[141] Based on the angiographic properties of ICG, it could play a role in determining vascular clamping during nephrectomy.[142,143] However, for tumor imaging NIR fluorescence imaging with ICG showed inconsistent results. One study compared the fluorescent signal with histologic findings in 100 patients undergoing partial nephrectomies, and showed that the ICG pattern (hypofluorescent, isofluorescent, or afluorescent) was insufficient to distinguish benign from malignant renal lesions.[144]

5.2 | How to use it

As summarized in Table 1, we recommend 10 mg, 2.5 mg and 0.25 mg/kg ICG injection intravenously for good intraoperative visibility of liver tumors, adrenal tumors and peritoneal metastases, respectively. Intraoperative injection is optimal for detection of peritoneal metastases and adrenal tumors, although for detection of liver tumors it is preferable to inject ICG 24 h before surgery.

6 | VISUALIZATION OF VITAL STRUCTURES

Currently, no good intraoperative imaging techniques are available for both biliary duct and ureter visualization. Intraoperative cholangiography is sometimes used for enhanced bile duct identification. Two disadvantages of this technique are the exposition of radiation to the patients and health care personnel and the chance of causing bile duct injuries by bile duct cannulation.[145,146] Other techniques such as ureteral stenting is sometimes performed to visualize the ureter. However, the benefit is currently questionable and it is also associated

with a risk of ureteral injury.[147,148] NIR fluorescence imaging with ICG and MB is used for both biliary and ureter mapping, based on their clearance characteristics.[7]

6.1 | Clinical applications

6.1.1 | Biliary duct

During laparoscopic cholecystectomy, nowadays one of the most performed surgeries, it is important to visualize the so-called critical view of safety. This ensures that the cystic duct has been identified correctly. Still, due to anatomical variations, the cystic duct could be misidentified by the common hepatic duct or the common bile duct. Misidentification, with a reported incidence ranging from 0.08% to 1.5%, is accomplished with a morbidity up to 21% and high healthcare costs.[149–152] The use of intravenously ICG injection for identification of the bile ducts with NIR fluorescence cholangiography was evaluated in 30 studies, which showed a pooled cystic duct identification in 1019/1050 (97%) patients.[140,153–181] Although, the biliary ducts could be very well visualized, the diminished visualization of the bile ducts in minority of the patients, could be caused by inflammatory tissue or fatty peritoneum (in obese patients) covering the biliary ducts, which hampered the penetration of NIR light.[174,176] In a pilot study it was recently discovered that directly injection of ICG into the gallbladder shows low fluorescence signals in the liver and seems also feasible, especially in case of severe cholecystitis.[182]

Summary of findings

Before starting with NIR fluorescence cholangiography, 5 mg ICG should be prepared according to a recent optimal dose study of our group.[183] Administering ICG directly prior to surgery results in highly fluorescent liver tissue, which may hamper identification of bile ducts. Therefore, ICG has to be injected intravenously 3-7 h before surgery for optimal bile duct to liver contrast, resulting in a better bile duct discrimination. For elective cholecystectomy, which is sometimes part of oncologic surgery (in case of cholangio- or pancreatic-carcinoma), this approach is feasible. Five studies showed that with this dose the cystic duct beginning to became

fluorescent around 30 to 40 min after intravenous ICG injection.[158,159,169,170,176]

In general, during cholecystectomy it is important to obtain the critical view of safety: visibility of the cystic duct and cystic artery entering the gallbladder. After preparation of the gallbladder hilum both medially and laterally, critical view could be achieved by retracting the gallbladder caudo-medially and exposing the triangle of Calot (Figure 4). If the cystic duct was detected, ICG could also be administrated again to visualize the cystic artery. It is important to realize that after a second ICG administration, the liver will become again highly fluorescent. After detection of both the cystic duct and cystic artery, these structures could be transected and the gallbladder could be removed.

6.1.2 | Ureter

Ureter injuries were seen in minority of the cases during colorectal surgery, with a reported incidence varying from 0.15% to 0.66% for open and laparoscopic procedures, respectively.[184] Although the incidence seems low, ureteral injuries are associated with a significant morbidity. The use of intraoperative ureter visualization with NIR fluorescence imaging was evaluated in six studies, of which four studies used ICG and two used MB as contrast agents.[185–190] ICG was used in three studies during robotic surgery to detect the level of the ureteral stenosis in a population varying from 7 to 25 patients. In these studies ICG was injected both through the ureteral catheter, of which only the tip was inserted into the ureteral orifice, or in the renal pelvis.

Summary of findings

We prefer MB above ICG as a NIR fluorescent contrast agent for detection of the ureter, because MB is cleared via the kidneys and could therefore intravenously injected easily. Verbeek et al[190] showed that in 12 patients both ureters could be detected 10 min after infusion of MB, whereas Al Taher et al[185] detected both ureters in only a half of the patients (5 out of 10). Verbeek et al[190] injected MB intraoperatively after visualization of the ureters. However, this approach is not comparable to clinical practice. Therefore we recommend to inject MB intravenously after first incision was made (open surgery) or after
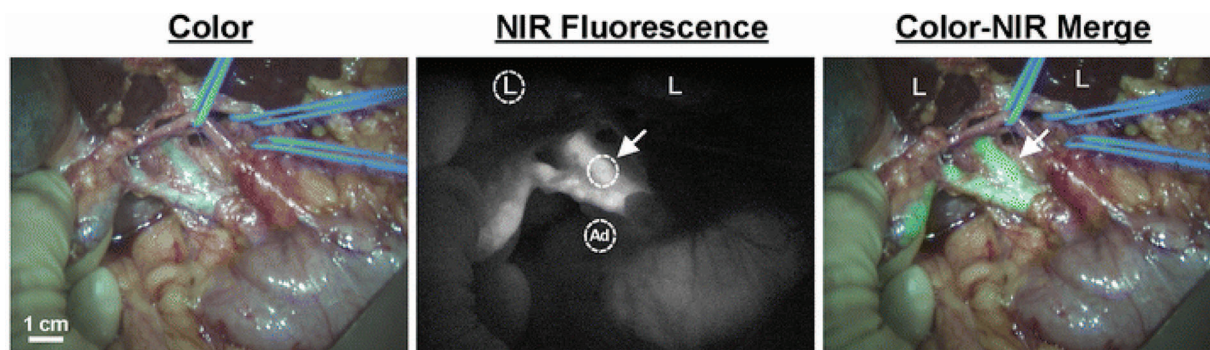
FIGURE 4 Example of bile duct imaging using ICG 24 h after injection. The position of the common bile duct was indicated by the arrow; the liver by L; and surrounding adipose tissue by Ad. Adapted and reprinted by permission from Springer Nature: Surgical Endoscopy[171] © 2014
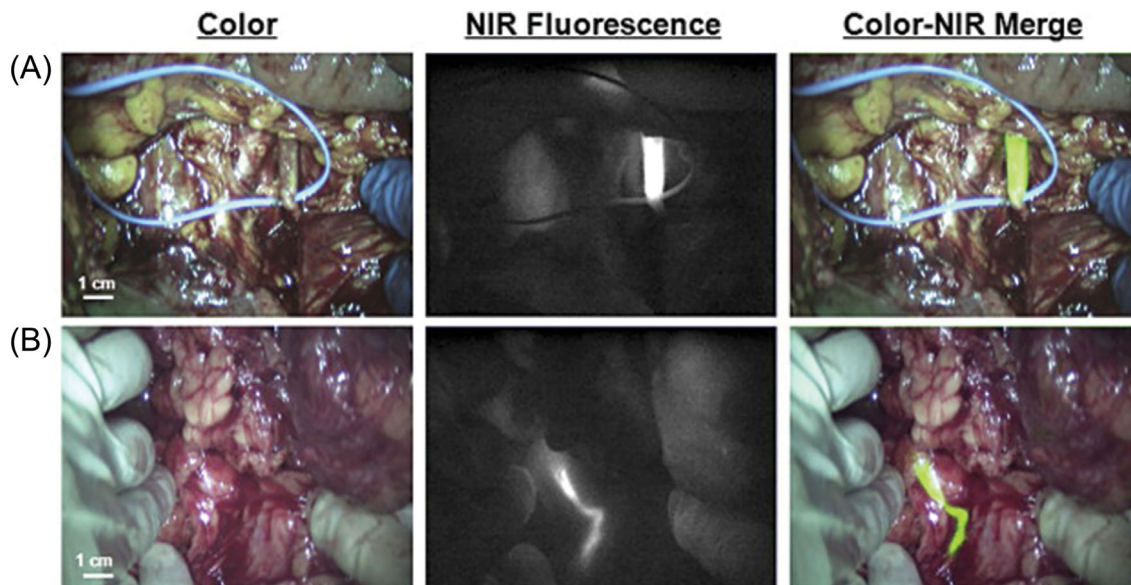
FIGURE 5 Example of ureter imaging using MB. Upper panel: NIRF image of right ureter, 45 min after MB administration. Lower panel: NIRF image of right ureter, covered by blood and tissue. Reprinted by permission from Elsevier: The Journal of Urology[190] © 2013

introduction of the first trocars (laparoscopic surgery). Based on both studies, 0.25 mg/kg MB could be injected, after which the ureters will become visible from 10 up to 60 min, as illustrated in Figure 5. A disadvantage of MB is that it is fluorescent at approximately 700 nm, which is subject to higher absorption and more nonspecific background fluorescence. A novel dye, ZW800-1, was therefore developed. This dye is fluorescent at 800 nm, exclusively cleared via the kidneys.

6.2 | How to use it

To summarize, ICG could be used for biliary duct imaging, whereas MB is preferable for ureter mapping. Optimal doses and injection times are 5 mg 3-7 h before surgery, and 0.25 mg/kg intraoperatively, respectively (Table 1).

7 | TISSUE PERFUSION

Restoring normal functioning and tissue healing after surgical intervention is, among others, critically dependent on tissue perfusion. Insufficient perfusion with oxygenated blood could result in ischemia and subsequent tissue damage. An important clinical problem is anastomotic leakage, which is one of the most serious complication after gastrointestinal surgery.[191,192] Large retrospective cohort studies showed leakage rates up to 19% in case of colorectal surgery.[192] Today, surgeons have to evaluate the anastomotic perfusion by inspection, which is a subjective method and difficult to quantify.[193] Different techniques have been used to evaluate the anastomotic perfusion, however none of them are currently common used in clinical practice, due to their disadvantages.[194]

Intraoperative evaluation of liver perfusion is also a clinical relevant issue, especially for determining the effect of the resection on the liver function, however currently no good intraoperative tools are available. Some studies suggests the use of contrast enhanced ultrasound, as an additional tool for resection planning.[195,196] Due to the characteristic of ICG binding to plasma proteins, it will mainly remain intravascular after intravenously injection, which makes it a perfect candidate for perfusion imaging.

7.1 | Clinical applications

7.1.1 | Anastomotic bowel perfusion

As the introduction of NIR fluorescence imaging, 11 clinical studies reported the use of ICG as a NIR fluorescent agent in evaluation of the esophagogastric anastomosis.[24,194,197–205] One study compared the anastomotic leakage rate in perfusion detection both with and without the use of ICG fluorescence imaging, which resulted in reducing the rate from 20% to 0%.[205] Twenty-one clinical trials reported the use of ICG as a NIR fluorescence agent with different imaging systems in intraoperative evaluation of colorectal anastomoses.[180,206–225] ICG was often injected after anastomotic site selection to evaluate the effect of ICG in selecting the correct anastomotic site. This resulted in the change of surgical plan between 3.7% and 40%. Some studies also evaluated the rate of the AL with using ICG and it was shown in a recent systematic review that the rate of AL decreases from 8.5% to 3.3% in the group which used ICG.[226] On the other hand, a case-matched retrospective study in 346 patients did not show a significant decline in AL (7.5% vs 6.4%), although the anastomotic site was changed in 5% of the patients.[214]

Summary of findings

Based on the above mentioned studies we recommend the following approach. First of all, normal surgical procedure could be started according to standard of care. Before performing the anastomosis, 2.5 mg of ICG dye can be injected intravenously, which is based on the doses used in most of the clinical trials.[197–200,202,203] However, most studies in colorectal surgery used ICG injection doses varying from 0.2 to 0.5 mg/kg.[206,213,221,223,224] Nevertheless, it was shown that the colorectal anastomotic perfusion could also be visualized by using a much lower and less toxic dose (2.5 mg), which is in concordance with the optimal dose used for evaluation gastroesophageal anastomotic perfusion.[210,212] Hence, we recommend an intravenously injection of 2.5 mg ICG for both types of anastomoses. Within 60 s the vasculature will be visible and the anastomotic site can be visualized with NIR fluorescence imaging.[209,210,212,215,223] If the fluorescence signal starts to fade, another bolus of 2.5 mg ICG can be injected to evaluate the perfusion for a second look (>15 min after first injection). If a good perfusion was detected with NIR fluorescence imaging, the procedure could be finished as usual.

7.1.2 | Hepatic perfusion during liver segmentectomy

Due to the complex liver anatomy, liver surgery is only performed in high volume centers. Especially, during oncologic surgery, it is difficult to determine the resection margins and to estimate the remnant liver volume in order to achieve the optimal balance between cancer curability and postoperative hepatic function. The portal and hepatic veins are the important anatomical landmarks used for resection planning. Seven studies evaluated the use of ICG for determining the resection planes during liver surgery.[104,110,117,164,227–229] In 89% to 100% of the performed surgeries, the resection lines could be easily visualized.

Summary of findings

After clamping of the selected portal branch, ICG could be injected, resulting in highlighted liver, except of the less-perfused part of the liver. Two methods of injection (portal vein and peripheral vein) were evaluated. The used doses of ICG varied from 1.25 mg to 0.5 mg/kg.[104,110,117,164,227–229] However, Inoue et al[228] showed comparable results of portal vein and peripheral vein injection with 2.5 mg ICG, which we therefore recommend as the optimal dose. Intraportal ICG injection could be performed under ultrasonic guidance after clamping the proximal portal pedicle. An alternative for portal injection is an intravenously (in a peripheral vein) ICG injection after clamping of the selected portal vein, which we prefer during laparoscopic surgery, due to the technical difficulties with portal injection. A disadvantage of intravenously ICG injection is the lower concentration of ICG available than using the intraportal injection method.[228] The liver segments become fluorescent after 1-2 min.[104,227]

7.2 | How to use it

For optimal evaluation of anastomotic bowel and liver segment perfusion a 2.5 mg intravenously injection of ICG is recommended. After intraoperative injection, the vasculature becomes visible after approximately one to 2 min (Table 1).

8 | DISCUSSION AND FUTURE PERSPECTIVES

NIR fluorescence imaging has been widely evaluated during the past decades. Several clinical studies have been performed with different conditions and therapeutic doses of contrast agents. Hence, it may be difficult for surgeons to directly apply these new techniques in daily practice, although the technique itself is fairly straightforward and has a limited learning curve. This review focussed on its application with the currently only available contrast agents, ICG and MB, during oncologic abdominal surgery, of which a summary was given in Table 1. We evaluated the timing of the injection, the injection locations, and the dose of contrast agents, which could guide the surgeon for intraoperative use of the different applications of NIR fluorescence imaging in abdominal oncologic surgery.

The use of ICG, contributes to a better visibility of sentinel lymph nodes, biliary ducts and tissue perfusion, than current image modalities or surgeons visual/tactical feedback. Furthermore, liver tumors could be easily identified with ICG, because of its clearing by the liver, whereas it is not specific for other types of solid abdominal tumors in the abdomen, such as pancreatic and renal tumors.[140,144] Moreover, we have shown that intraoperative visualization of peritoneal metastases and adrenal tumors using ICG is feasible and could therefore be used as an additional intraoperative image modality until specific tumor targets are available. Today, no evidence is available for intraoperative visualization of nerves, which is important during colorectal surgery, using ICG due to its non-specificity.[230–232] Therefore, diverse other nerve specific contrast agents are currently being investigated.[233–237]

MB was evaluated for ureter detection, however its clinical use during abdominal surgery, would be limited subject due to higher absorption and more nonspecific background fluorescence. Hence, a specific antibody binding to a fluorophore, ZW800-1, has been evaluated and showed better ureter visibility than MB in preclinically testing.[238] Moreover, it was also described that MB could be useful in abdominal surgery for detection of neuroendocrine tumors. However, the evidence is limited to one preclinical mice study and a case report of a patient with a paraganglioma, and should therefore be further validated in new studies.[239,240]

To improve the tumor visibility during oncologic surgery, (new) NIR fluorophores, such as IRDye-800CW, were combined with tumor-specific targets as described by Haque et al.[241] Diverse specific tumor-specific fluorophores have been investigated during the last years, for instance in patients with colorectal cancer (during endoscopy), ovarian cancer, renal cell carcinoma, and peritonitis carcinomatosa.[242–246] Currently, more clinical trials in patients with

pancreatic, colorectal and renal cancer are underway (NCT02743975, NCT02317705, NCT01778933, NCT02973672).

Although we have shown the great progress made using NIR fluorescence imaging, it also has his limitations. The most important drawback is the lack of quantitative comparison of fluorescence signals in the currently published studies. Especially, for evaluation of anastomotic bowel perfusion, most of them did not take into account the over-time diffusion of the used NIR fluorophore, resulting in an overestimation of the fluorescence signal in vascularized areas. Diana et al[247–250] developed a quantitative software based analysis which calculates the stiffness of the slope of the fluorescence signal to reach the peak intensity, given the fact this is the most important perfusion marker. Based on those parameters, a virtual bowel perfusion cartography is created, which could be superimposed on the white light images, resulting in a nearly real-time quantitative perfusion image, as shown in Figure 6.

Today, NIR fluorescence imaging is performed in the classic first NIR window, between 650 and 950 nm. The penetration depth of NIR light in the first NIR window is up to 1 cm and therefore limited for detection of superficial lesions, however it could even be useful for intraoperative margin assessment.[123] NIR fluorescence imaging systems, capable of imaging in the second NIR or shortwave infrared window (1000-1700 nm), will allow more in depth visibility of structures.

In conclusion, ICG and MB are relatively safe and sensitive non-specific fluorophores, which have been widely evaluated in NIR fluorescence imaging. In the nearby future, more specific tumor targets will be evaluated and used in clinical practice, which will provide new opportunities in the field of abdominal surgery.

CONFLICTS OF INTEREST

All authors declare that there is no conflict of interest.

ORCID

Labrinus van Manen (iD) http://orcid.org/0000-0003-2287-107X
Alexander L. Vahrmeijer (iD) http://orcid.org/0000-0001-9370-0011

REFERENCES

1. Torre LA, Bray F, Siegel RL, et al. Global cancer statistics, 2012. _CA Cancer J Clin_. 2015;65:87–108.
2. Kubben PL, ter Meulen KJ, Schijns OE, et al. Intraoperative MRI-guided resection of glioblastoma multiforme: a systematic review. _Lancet Oncol_. 2011;12:1062–1070.
3. Tilly C, Lefevre JH, Svrcek M, et al. R1 rectal resection: look up and don't look down. _Ann Surg_. 2014;260:794–799.
4. Khan MA, Hakeem AR, Scott N, Saunders RN. Significance of R1 resection margin in colon cancer resections in the modern era. _Colorectal Dis_. 2015;17:943–953.
5. Mondal SB, Gao S, Zhu N, et al. Real-time fluorescence image-guided oncologic surgery. _Adv Cancer Res_. 2014;124:171–211.
6. DSouza AV, Lin H, Henderson ER, et al. Review of fluorescence guided surgery systems: identification of key performance capabilities beyond indocyanine green imaging. _J Biomed Opt_. 2016;21: 080901.
7. Gioux S, Choi HS, Frangioni JV. Image-guided surgery using invisible near-infrared light: fundamentals of clinical translation. _Mol Imaging_. 2010;9:237–255.
8. Handgraaf HJ, Verbeek FP, Tummers QR, et al. Real-time near-infrared fluorescence guided surgery in gynecologic oncology: a review of the current state of the art. _Gynecol Oncol_. 2014;135:606–613.
9. Chance B. Near-infrared images using continuous, phase-modulated, and pulsed light with quantitation of blood and blood oxygenation. _Ann NY Acad Sci_. 1998;838:29–45.
10. Frangioni JV. In vivo near-infrared fluorescence imaging. _Curr Opin Chem Biol_. 2003;7:626–634.
11. Stammes MA, Bugby SL, Porta T, et al. Modalities for image- and molecular-guided cancer surgery. _Br J Surg_. 2018;105:e69–e83.
12. Stummer W, Pichlmeier U, Meinel T, et al. Fluorescence-guided surgery with 5-aminolevulinic acid for resection of malignant glioma: a randomised controlled multicentre phase III trial. _Lancet Oncol_. 2006;7:392–401.
13. Shimizu S, Kamiike W, Hatanaka N, et al. New method for measuring ICG Rmax with a clearance meter. _World J Surg_. 1995;19:113–118.
14. Benya R, Quintana J, Brundage B. Adverse reactions to indocyanine green: a case report and a review of the literature. _Cathet Cardiovasc Diagn_. 1989;17:231–233.
15. Ginimuge PR, Jyothi SD. Methylene blue: revisited. _J Anaesthesiol Clin Pharmacol_. 2010;26:517–520.
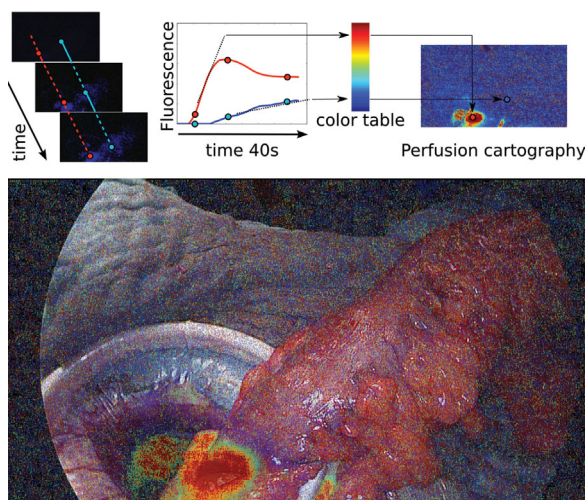
FIGURE 6 The concept of quantitative fluorescence measurements (Fluorescence-based Enhanced Reality = FLER) for determining the bowel perfusion. Upper panel: The fluorescence signal is analyzed during 40 s after intravenous administration of ICG. Using specific software (VR-PERFUSION, IRCAD; France) the slope of the fluorescence time-to-peak is computed and converted to color codes, resulting in a virtual perfusion cartography. Lower panel: The white light image is combined with the perfusion cartography, creating an augmented reality view of the bowel perfusion at the resection site

16. Valsecchi ME, Silbermins D, de Rosa N, et al. Lymphatic mapping and sentinel lymph node biopsy in patients with melanoma: a meta-analysis. *J Clin Oncol*. 2011;29:1479–1487.

17. He PS, Li F, Li GH, et al. The combination of blue dye and radioisotope versus radioisotope alone during sentinel lymph node biopsy for breast cancer: a systematic review. *BMC Cancer*. 2016;16:107.

18. Hayashi H, Ochiai T, Mori M, et al. Sentinel lymph node mapping for gastric cancer using a dual procedure with dye- and gamma probe-guided techniques. *J Am Coll Surg*. 2003;196:68–74.

19. Levenback CF, van der Zee AG, Rob L, et al. Sentinel lymph node biopsy in patients with gynecologic cancers Expert panel statement from the International Sentinel Node Society Meeting, February 21, 2008. *Gynecol Oncol*. 2009;114:151–156.

20. Dubecz A, Gall I, Solymosi N, et al. Temporal trends in long-term survival and cure rates in esophageal cancer: a SEER database analysis. *J Thoracic Oncol*. 2012;7:443–447.

21. Lerut T, Nafteux P, Moons J, et al. Three-field lymphadenectomy for carcinoma of the esophagus and gastroesophageal junction in 174 R0 resections: impact on staging, disease-free survival, and outcome: a plea for adaptation of TNM classification in upper-half esophageal carcinoma. *Ann Surg*. 2004;240:962–972.

22. Nishihira T, Hirayama K, Mori S. A prospective randomized trial of extended cervical and superior mediastinal lymphadenectomy for carcinoma of the thoracic esophagus. *Am J Surg*. 1998;175:47–51.

23. Peyre CG, Hagen JA, DeMeester SR, et al. The number of lymph nodes removed predicts survival in esophageal cancer: an international study on the impact of extent of surgical resection. *Ann Surg*. 2008;248:549–556.

24. Kubota K, Yoshida M, Kuroda J, et al. Application of the HyperEye medical system for esophageal cancer surgery: a preliminary report. *Surg Today*. 2013;43:215–220.

25. Yuasa Y, Seike J, Yoshida T, et al. Sentinel lymph node biopsy using intraoperative indocyanine green fluorescence imaging navigated with preoperative CT lymphography for superficial esophageal cancer. *Ann Surgical Oncol*. 2012;19:486–493.

26. Hachey KJ, Gilmore DM, Armstrong KW, et al. Safety and feasibility of near-infrared image-guided lymphatic mapping of regional lymph nodes in esophageal cancer. *J Thorac Cardiovasc Surg*. 2016;152:546–554.

27. Fujita T, Seshimo A, Kameoka S. Detection of sentinel nodes in gastric cancer by indocyanine green fluorescence imaging. *Hepato-gastroenterology*. 2012;59:2213–2216.

28. Kinami S, Oonishi T, Fujita J, et al. Optimal settings and accuracy of indocyanine green fluorescence imaging for sentinel node biopsy in early gastric cancer. *Oncol Lett*. 2016;11:4055–4062.

29. Kusano M, Tajima Y, Yamazaki K, et al. Sentinel node mapping guided by indocyanine green fluorescence imaging: a new method for sentinel node navigation surgery in gastrointestinal cancer. *Dig Surg*. 2008;25:103–108.

30. Miyashiro I, Miyoshi N, Hiratsuka M, et al. Detection of sentinel node in gastric cancer surgery by indocyanine green fluorescence imaging: comparison with infrared imaging. *Ann Surg Oncol*. 2008;15:1640–1643.

31. Miyashiro I, Kishi K, Yano M, et al. Laparoscopic detection of sentinel node in gastric cancer surgery by indocyanine green fluorescence imaging. *Surg Endosc*. 2011;25:1672–1676.

32. Tajima Y, Murakami M, Yamazaki K, et al. Sentinel node mapping guided by indocyanine green fluorescence imaging during laparo-scopic surgery in gastric cancer. *Ann Surg Oncol*. 2010;17:1787–1793.

33. Takahashi N, Nimura H, Fujita T, et al. Laparoscopic sentinel node navigation surgery for early gastric cancer: a prospective multicenter trial. *Langenbeck's Arch Surg*. 2017;402:27–32.

34. Yoshida M, Kubota K, Kuroda J, et al. Indocyanine green injection for detecting sentinel nodes using color fluorescence camera in the laparoscopy-assisted gastrectomy. *J Gastroenterol Hepatol*. 2012;27:29–33.

35. Tummers QR, Boogerd LS, de Steur WO, et al. Near-infrared fluorescence sentinel lymph node detection in gastric cancer: a pilot study. *World J Gastroenterol*. 2016;22:3644–3651.

36. Tajima Y, Yamazaki K, Masuda Y, et al. Sentinel node mapping guided by indocyanine green fluorescence imaging in gastric cancer. *Ann Surg*. 2009;249:58–62.

37. Bok GH, Kim YJ, Jin SY, et al. Endoscopic submucosal dissection with sentinel node navigation surgery for early gastric cancer. *Endoscopy*. 2012;44:953–956.

38. Bembenek AE, Rosenberg R, Wagler E, et al. Sentinel lymph node biopsy in colon cancer: a prospective multicenter trial. *Ann Surg*. 2007;245:858–863.

39. Andersen HS, Bennedsen ALB, Burgdorf SK, et al. In vivo and ex vivo sentinel node mapping does not identify the same lymph nodes in colon cancer. *Int J Colorectal Dis* 2017;32:983–990.

40. Ankersmit M, van der Pas MH, van Dam DA, Meijerink WJ. Near infrared fluorescence lymphatic laparoscopy of the colon and mesocolon. *Colorectal Dis*. 2011;13:70–73.

41. Cahill RA, Anderson M, Wang LM, et al. Near-infrared (NIR) laparoscopy for intraoperative lymphatic road-mapping and sentinel node identification during definitive surgical resection of early-stage colorectal neoplasia. *Surg Endosc*. 2012;26:197–204.

42. Hirche C, Mohr Z, Kneif S, et al. Ultrastaging of colon cancer by sentinel node biopsy using fluorescence navigation with indocyanine green. *Int J Colorectal Dis*. 2012;27:319–324.

43. van der Pas MH, Ankersmit M, Stockmann HB, et al. Laparoscopic sentinel lymph node identification in patients with colon carcinoma using a near-infrared dye: description of a new technique and feasibility study. *J Laparoendosc Adv Surg Tech A*. 2013;23:367–371.

44. Noura S, Ohue M, Seki Y, et al. Feasibility of a lateral region sentinel node biopsy of lower rectal cancer guided by indocyanine green using a near-infrared camera system. *Ann Surg Oncol*. 2010;17:144–151.

45. Currie AC, Brigic A, Thomas-Gibson S, et al. A pilot study to assess near infrared laparoscopy with indocyanine green (ICG) for intraoperative sentinel lymph node mapping in early colon cancer. *Eur J Surg Oncol*. 2017;43:2044–2051.

46. Handgraaf HJ, Boogerd LS, Verbeek FP, et al. Intraoperative fluorescence imaging to localize tumors and sentinel lymph nodes in rectal cancer. *Minim Invasive Ther Allied Technol*. 2016;25:48–53.

47. Hurle R, Naspro R. Pelvic lymphadenectomy during radical cystec-tomy: a review of the literature. *Surg Oncol*. 2010;19:208–220.

48. Polom W, Markuszewski M, Cytawa W, et al. Fluorescent versus radioguided lymph node mapping in bladder cancer. *Clin Genitourin Cancer*. 2017;15:e405–e409.

49. Schaafsma BE, Verbeek FP, Elzevier HW, et al. Optimization of sentinel lymph node mapping in bladder cancer using near-infrared fluorescence imaging. *J Surg Oncol*. 2014;110:845–850.

50. Manny TB, Hemal AK. Fluorescence-enhanced robotic radical cystectomy using unconjugated indocyanine green for pelvic lymphangiography, tumor marking, and mesenteric angiography: the initial clinical experience. *Urology*. 2014;83:824–829.

51. Siegel RL, Miller KD, Jemal A. Cancer statistics, 2017. *CA Cancer J Clin*. 2017;67:7–30.

52. Cagiannos I, Karakiewicz P, Eastham JA, et al. A preoperative nomogram identifying decreased risk of positive pelvic lymph nodes in patients with prostate cancer. *J Urol*. 2003;170:1798–1803.

53. Hansen J, Rink M, Bianchi M, et al. External validation of the updated Briganti nomogram to predict lymph node invasion in prostate cancer patients undergoing extended lymph node dissection. *Prostate*. 2013;73:211–218.

54. Chennamsetty A, Zhumkhawala A, Tobis SB, et al. Lymph node fluorescence during robot-assisted radical prostatectomy with

indocyanine green: prospective dosing analysis. *Clin Genitourin Cancer*. 2017;15:e529–e534.

55. Morozov AO, Alyaev YG, Rapoport LM, et al. Near-infrared fluorescence with indocyanine green for diagnostics in urology: initial experience. *Urologia*. 2017;84:197–202.

56. Nguyen DP, Huber PM, Metzger TA, et al. A specific mapping study using fluorescence sentinel lymph node detection in patients with intermediate- and high-risk prostate cancer undergoing extended pelvic lymph node dissection. *Eur Urol*. 2016;70:734–737.

57. Hruby S, Englberger C, Lusuardi L, et al. Fluorescence guided targeted pelvic lymph node dissection for intermediate and high risk prostate cancer. *J Urol*. 2015;194:357–363.

58. Ramirez-Backhaus M, Mira Moreno A, Gomez Ferrer A, et al. Indocyanine green guided pelvic lymph node dissection: an efficient technique to classify the lymph node status of patients with prostate cancer who underwent radical prostatectomy. *J Urol*. 2016;196: 1429–1435.

59. van den Berg NS, Buckle T, KleinJan GH, et al. Multispectral fluorescence imaging during robot-assisted laparoscopic sentinel node biopsy: a first step towards a fluorescence-based anatomic roadmap. *Eur Urol*. 2017;72:110–117.

60. KleinJan GH, van den Berg NS, de Jong J, et al. Multimodal hybrid imaging agents for sentinel node mapping as a means to (re)connect nuclear medicine to advances made in robot-assisted surgery. *Eur J Nucl Med Mol Imaging*. 2016;43:1278–1287.

61. Yuen K, Miura T, Sakai I, et al. Intraoperative fluorescence imaging for detection of sentinel lymph nodes and lymphatic vessels during open prostatectomy using indocyanine green. *J Urol*. 2015;194: 371–377.

62. Manny TB, Patel M, Hemal AK. Fluorescence-enhanced robotic radical prostatectomy using real-time lymphangiography and tissue marking with percutaneous injection of unconjugated indocyanine green: the initial clinical experience in 50 patients. *Eur Urol*. 2014;65:1162–1168.

63. Jeschke S, Lusuardi L, Myatt A, et al. Visualisation of the lymph node pathway in real time by laparoscopic radioisotope- and fluorescence-guided sentinel lymph node dissection in prostate cancer staging. *Urology*. 2012;80:1080–1086.

64. van der Poel HG, Buckle T, Brouwer OR, et al. Intraoperative laparoscopic fluorescence guidance to the sentinel lymph node in prostate cancer patients: clinical proof of concept of an integrated functional imaging approach using a multimodal tracer. *Eur Urol*. 2011;60:826–833.

65. Averette HE, Nguyen HN, Donato DM, et al. Radical hysterectomy for invasive cervical cancer. A 25-year prospective experience with the Miami technique. *Cancer*. 1993;71:1422–1437.

66. Di Stefano AB, Acquaviva G, Garozzo G, et al. Lymph node mapping and sentinel node detection in patients with cervical carcinoma: a 2-year experience. *Gynecol Oncol*. 2005;99:671–679.

67. Crane LM, Themelis G, Pleijhuis RG, et al. Intraoperative multispectral fluorescence imaging for the detection of the sentinel lymph node in cervical cancer: a novel concept. *Molecul Imaging Biol*. 2011; 13:1043–1049.

68. Buda A, Bussi B, Di Martino G, et al. Sentinel lymph node mapping with near-infrared fluorescent imaging using indocyanine green: a new tool for laparoscopic platform in patients with endometrial and cervical cancer. *J Minim Invasive Gynecol*. 2016;23:265–269.

69. Laios A, Volpi D, Tullis ID, et al. A prospective pilot study of detection of sentinel lymph nodes in gynaecological cancers using a novel near infrared fluorescence imaging system. *BMC Res Notes*. 2015;8:608.

70. Beavis AL, Salazar-Marioni S, Sinno AK, et al. Sentinel lymph node detection rates using indocyanine green in women with early-stage cervical cancer. *Gynecol Oncol*. 2016;143:302–306.

71. Buda A, Di Martino G, Vecchione F, et al. Optimizing strategies for sentinel lymph node mapping in early-stage cervical and endometrial

cancer: comparison of real-time fluorescence with indocyanine green and methylene blue. *Int J Gynecol Cancer*. 2015;25:1513–1518.

72. Buda A, Dell'Anna T, Vecchione F, et al. Near-infrared sentinel lymph node mapping with indocyanine green using the VITOM II ICG exoscope for open surgery for gynecologic malignancies. *J Minim Invasive Gynecol*. 2016;23:628–632.

73. Buda A, Papadia A, Zapardiel I, et al. From conventional radiotracer Tc-99(m) with blue dye to indocyanine green fluorescence: a comparison of methods towards optimization of sentinel lymph node mapping in early stage cervical cancer for a laparoscopic approach. *Ann Surg Ooncol*. 2016;23:2959–2965.

74. Imboden S, Papadia A, Nauwerk M, et al. A comparison of radiocolloid and indocyanine green fluorescence imaging, sentinel lymph node mapping in patients with cervical cancer undergoing laparoscopic surgery. *Ann Surg Oncol*. 2015;22:4198–4203.

75. Paredes P, Vidal-Sicart S, Campos F, et al. Role of ICG-99mTc-nanocolloid for sentinel lymph node detection in cervical cancer: a pilot study. *Eur J Nucl Med Mol Imaging*. 2017;44:1853–1861.

76. Di Martino G, Crivellaro C, De Ponti E, et al. Indocyanine green versus radiotracer with or without blue dye for sentinel lymph node mapping in stage >IB1 cervical cancer (>2 cm). *J Minim Invasive Gynecol*. 2017;24:954–959.

77. Lopez Labrousse MI, Frumovitz M, Guadalupe Patrono M, Ramirez PT. Sentinel lymph node mapping in minimally invasive surgery: role of imaging with color-segmented fluorescence (CSF). *Gynecol Oncol*. 2017;146:676–677.

78. Jewell EL, Huang JJ, Abu-Rustum NR, et al. Detection of sentinel lymph nodes in minimally invasive surgery using indocyanine green and near-infrared fluorescence imaging for uterine and cervical malignancies. *Gynecol Oncol*. 2014;133:274–277.

79. Schaafsma BE, van der Vorst JR, Gaarenstroom KN, et al. Randomized comparison of near-infrared fluorescence lymphatic tracers for sentinel lymph node mapping of cervical cancer. *Gynecol Oncol*. 2012;127:126–130.

80. Rossi EC, Ivanova A, Boggess JF. Robotically assisted fluorescence-guided lymph node mapping with ICG for gynecologic malignancies: a feasibility study. *Gynecol Oncol*. 2012;124:78–82.

81. van der Vorst JR, Hutteman M, Gaarenstroom KN, et al. Optimization of near-infrared fluorescent sentinel lymph node mapping in cervical cancer patients. *Int J Gynecol Cancer*. 2011;21:1472–1478.

82. Furukawa N, Oi H, Yoshida S, et al. The usefulness of photodynamic eye for sentinel lymph node identification in patients with cervical cancer. *Tumori*. 2010;96:936–940.

83. Buda A, Di Martino G, De Ponti E, et al. Laparoscopic sentinel node mapping in cervical and endometrial malignancies: a case-control study comparing two near-infrared fluorescence systems. *J Minim Invasive Gynecol*. 2018;25:93–98.

84. Orr JW, Jr., Holloway RW, Orr PF, Holimon JL. Surgical staging of uterine cancer: an analysis of perioperative morbidity. *Gynecol Oncol*. 1991;42:209–216.

85. Abu-Rustum NR. Sentinel lymph node mapping for endometrial cancer: a modern approach to surgical staging. *J Natl Compr Canc Netw*. 2014;12:288–297.

86. Yamagami W, Susumu N, Kataoka F, et al. A comparison of dye versus fluorescence methods for sentinel lymph node mapping in endometrial cancer. *Int J Gynecol Cancer*. 2017;27:1517–1524.

87. Rossi EC, Jackson A, Ivanova A, Boggess JF. Detection of sentinel nodes for endometrial cancer with robotic assisted fluorescence imaging: cervical versus hysteroscopic injection. *Int J Gynecol Cancer*. 2013;23:1704–1711.

88. Papadia A, Zapardiel I, Bussi B, et al. Sentinel lymph node mapping in patients with stage I endometrial carcinoma: a focus on bilateral mapping identification by comparing radiotracer Tc99m with blue dye versus indocyanine green fluorescent dye. *J Cancer Res Clin Oncol*. 2017;143:475–480.

89. Paley PJ, Veljovich DS, Press JZ, et al. A prospective investigation of fluorescence imaging to detect sentinel lymph nodes at robotic-assisted endometrial cancer staging. *Am J Obstet Gynecol*. 2016;215:117.e111–117.e117.

90. Martinelli F, Ditto A, Bogani G, et al. Laparoscopic sentinel node mapping in endometrial cancer after hysteroscopic injection of indocyanine green. *J Minim Invasive Gynecol*. 2017;24:89–93.

91. Holloway RW, Ahmad S, Kendrick JE, et al. A prospective cohort study comparing colorimetric and fluorescent imaging for sentinel lymph node mapping in endometrial cancer. *Ann Surg Oncol*. 2017;24:1972–1979.

92. Holloway RW, Bravo RA, Rakowski JA, et al. Detection of sentinel lymph nodes in patients with endometrial cancer undergoing robotic-assisted staging: a comparison of colorimetric and fluorescence imaging. *Gynecol Oncol*. 2012;126:25–29.

93. Hagen B, Valla M, Aune G, et al. Indocyanine green fluorescence imaging of lymph nodes during robotic-assisted laparoscopic operation for endometrial cancer. A prospective validation study using a sentinel lymph node surgical algorithm. *Gynecol Oncol*. 2016;143:479–483.

94. Geppert B, Lonnerfors C, Bollino M, et al. A study on uterine lymphatic anatomy for standardization of pelvic sentinel lymph node detection in endometrial cancer. *Gynecol Oncol*. 2017;145:256–261.

95. Eriksson AG, Beavis A, Soslow RA, et al. A comparison of the detection of sentinel lymph nodes using indocyanine green and near-infrared fluorescence imaging versus blue dye during robotic surgery in uterine cancer. *Int J Gynecol Cancer*. 2017;27:743–747.

96. Eriksson AG, Montovano M, Beavis A, et al. Impact of obesity on sentinel lymph node mapping in patients with newly diagnosed uterine cancer undergoing robotic surgery. *Ann Surg Oncol*. 2016;23:2522–2528.

97. Taskin S, Sukur YE, Altin D, et al. Laparoscopic near-infrared fluorescent imaging as an alternative option for sentinel lymph node mapping in endometrial cancer: a prospective study. *Int J Sur. (London, England)* 2017;47:13–17.

98. Buda A, Passoni P, Corrado G, et al. Near-infrared fluorescence-guided sentinel node mapping of the ovary with indocyanine green in a minimally invasive setting: a feasible study. *J Minim Invasive Gynecol*. 2017;24:165–170.

99. Matsumura Y, Maeda H. A new concept for macromolecular therapeutics in cancer chemotherapy: mechanism of tumoritropic accumulation of proteins and the antitumor agent smancs. *Cancer Res*. 1986;46:6387–6392.

100. Maeda H, Wu J, Sawa T, et al. Tumor vascular permeability and the EPR effect in macromolecular therapeutics: a review. *J Control Release*. 2000;65:271–284.

101. Ishizawa T, Masuda K, Urano Y, et al. Mechanistic background and clinical applications of indocyanine green fluorescence imaging of hepatocellular carcinoma. *Ann Surg Oncol*. 2014;21:440–448.

102. Boogerd LS, Handgraaf HJ, Lam HD, et al. Laparoscopic detection and resection of occult liver tumors of multiple cancer types using real-time near-infrared fluorescence guidance. *Surg Endosc*. 2017;31:952–961.

103. Handgraaf HJM, Boogerd LSF, Hoppener DJ, et al. Long-term follow-up after near-infrared fluorescence-guided resection of colorectal liver metastases: a retrospective multicenter analysis. *Eur J Surg Oncol*. 2017;43:1463–1471.

104. Aoki T, Yasuda D, Shimizu Y, et al. Image-guided liver mapping using fluorescence navigation system with indocyanine green for anatomical hepatic resection. *World J Surg*. 2008;32:1763–1767.

105. Yokoyama N, Otani T, Hashidate H, et al. Real-time detection of hepatic micrometastases from pancreatic cancer by intraoperative fluorescence imaging: preliminary results of a prospective study. *Cancer*. 2012;118:2813–2819.

106. Morita Y, Sakaguchi T, Unno N, et al. Detection of hepatocellular carcinomas with near-infrared fluorescence imaging using indocyanine green: its usefulness and limitation. *Int J Clin Oncol*. 2013;18:232–241.

107. Ishizuka M, Kubota K, Kita J, et al. Intraoperative observation using a fluorescence imaging instrument during hepatic resection for liver metastasis from colorectal cancer. *Hepatogastroenterology*. 2012;59:90–92.

108. Peloso A, Franchi E, Canepa MC, et al. Combined use of intraoperative ultrasound and indocyanine green fluorescence imaging to detect liver metastases from colorectal cancer. *HPB*. 2013;15:928–934.

109. Kudo H, Ishizawa T, Tani K, et al. Visualization of subcapsular hepatic malignancy by indocyanine-green fluorescence imaging during laparoscopic hepatectomy. *Surg Eendosc*. 2014;28:2504–2508.

110. Abo T, Nanashima A, Tobinaga S, et al. Usefulness of intraoperative diagnosis of hepatic tumors located at the liver surface and hepatic segmental visualization using indocyanine green-photodynamic eye imaging. *Eur J Surg Oncol*. 2015;41:257–264.

111. Shimada S, Ohtsubo S, Ogasawara K, Kusano M. Macro- and microscopic findings of ICG fluorescence in liver tumors. *World J Surg Oncol*. 2015;13:198.

112. Kawaguchi Y, Nagai M, Nomura Y, et al. Usefulness of indocyanine green-fluorescence imaging during laparoscopic hepatectomy to visualize subcapsular hard-to-identify hepatic malignancy. *J Surg Oncol*. 2015;112:514–516.

113. Kaibori M, Matsui K, Ishizaki M, et al. Intraoperative detection of superficial liver tumors by fluorescence imaging using indocyanine green and 5-aminolevulinic acid. *Anticancer Res*. 2016;36:1841–1849.

114. Zhang YM, Shi R, Hou JC, et al. Liver tumor boundaries identified intraoperatively using real-time indocyanine green fluorescence imaging. *J Cancer Res Clin Oncol*. 2017;143:51–58.

115. Takahashi H, Zaidi N, Berber E. An initial report on the intraoperative use of indocyanine green fluorescence imaging in the surgical management of liver tumorss. *J Surg Oncol*. 2016;114:625–629.

116. Masuda K, Kaneko J, Kawaguchi Y, et al. Diagnostic accuracy of indocyanine green fluorescence imaging and multidetector row computed tomography for identifying hepatocellular carcinoma with liver explant correlation. *Hepatol Res*. 2017;47:1299–1307.

117. Terasawa M, Ishizawa T, Mise Y, et al. Applications of fusion-fluorescence imaging using indocyanine green in laparoscopic hepatectomy. *Surg Endosc*. 2017;31:5111–5118.

118. Gotoh K, Yamada T, Ishikawa O, et al. A novel image-guided surgery of hepatocellular carcinoma by indocyanine green fluorescence imaging navigation. *J Surg Oncol*. 2009;100:75–79.

119. Uchiyama K, Ueno M, Ozawa S, et al. Combined use of contrast-enhanced intraoperative ultrasonography and a fluorescence navigation system for identifying hepatic metastases. *World J Surg*. 2010;34:2953–2959.

120. Ishizawa T, Fukushima N, Shibahara J, et al. Real-time identification of liver cancers by using indocyanine green fluorescent imaging. *Cancer*. 2009;115:2491–2504.

121. Tummers QR, Verbeek FP, Prevoo HA, et al. First experience on laparoscopic near-infrared fluorescence imaging of hepatic uveal melanoma metastases using indocyanine green. *Surg Innov*. 2015;22:20–25.

122. van der Vorst JR, Schaafsma BE, Hutteman M, et al. Near-infrared fluorescence-guided resection of colorectal liver metastases. *Cancer*. 2013;119:3411–3418.

123. Vahrmeijer AL, Hutteman M, van der Vorst JR, et al. Image-guided cancer surgery using near-infrared fluorescence. *Nat Rev Clin Oncol*. 2013;10:507–518.

124. Holzapfel K, Reiser-Erkan C, Fingerle AA, et al. Comparison of diffusion-weighted MR imaging and multidetector-row CT in the

detection of liver metastases in patients operated for pancreatic cancer. *Abd Imaging*. 2011;36:179–184.

125. Hariharan D, Constantinides VA, Froeling FE, et al. The role of laparoscopy and laparoscopic ultrasound in the preoperative staging of pancreatico-biliary cancers–A meta-analysis. *Eur J Surg Oncol*. 2010;36:941–948.

126. de Bree E, Koops W, Kroger R, et al. Peritoneal carcinomatosis from colorectal or appendiceal origin: correlation of preoperative CT with intraoperative findings and evaluation of interobserver agreement. *J Surg Oncol*. 2004;86:64–73.

127. Kuijpers AM, Mirck B, Aalbers AG, et al. Cytoreduction and HIPEC in the Netherlands: nationwide long-term outcome following the Dutch protocol. *Ann Surg Oncol*. 2013;20:4224–4230.

128. Al Rawahi T, Lopes AD, Bristow RE, et al. Surgical cytoreduction for recurrent epithelial ovarian cancer. *Cochrane Database Syst Rev*. 2013;Cd008765. https://doi.org/10.1002/14651858.CD008765.pub3

129. Liberale G, Vankerckhove S, Caldon MG, et al. Fluorescence imaging after indocyanine green injection for detection of peritoneal metastases in patients undergoing cytoreductive surgery for peritoneal carcinomatosis from colorectal cancer: a pilot study. *Ann Surg*. 2016;264:1110–1115.

130. Satou S, Ishizawa T, Masuda K, et al. Indocyanine green fluorescent imaging for detecting extrahepatic metastasis of hepatocellular carcinoma. *J Gastroenterol*. 2013;48:1136–1143.

131. Veys I, Pop FC, Vankerckhove S, et al. ICG-fluorescence imaging for detection of peritoneal metastases and residual tumoral scars in locally advanced ovarian cancer: a pilot study. *J Surg Oncol*. 2018;117:228–235.

132. Tummers QR, Hoogstins CE, Peters AA, et al. The value of intraoperative near-infrared fluorescence imaging based on en-hanced permeability and retention of indocyanine green: feasibility and false-positives in ovarian cancer. *PLoS ONE*. 2015;10:e0129766.

133. Gilly FN, Cotte E, Brigand C, et al. Quantitative prognostic indices in peritoneal carcinomatosis. *Eur J Surg Oncol*. 2006;32:597–601.

134. Janetschek G, Finkenstedt G, Gasser R, et al. Laparoscopic surgery for pheochromocytoma: adrenalectomy, partial resection, excision of paragangliomas. *J Urol*. 1998;160:330–334.

135. Kumar A, Hyams ES, Stifelman MD. Robot-assisted partial adrenalec-tomy for isolated adrenal metastasis. *J Endourol*. 2009;23: 651–654.

136. DeLong JC, Chakedis JM, Hosseini A, et al. Indocyanine green (ICG) fluorescence-guided laparoscopic adrenalectomy. *J Surg Oncol*. 2015;112:650–653.

137. Sound S, Okoh AK, Bucak E, et al. Intraoperative tumor localization and tissue distinction during robotic adrenalectomy using indoc-yanine green fluorescence imaging: a feasibility study. *Surg Endosc*. 2016;30:657–662.

138. Manny TB, Pompeo AS, Hemal AK. Robotic partial adrenalectomy using indocyanine green dye with near-infrared imaging: the initial clinical experience. *Urology*. 2013;82:738–742.

139. Colvin J, Zaidi N, Berber E. The utility of indocyanine green fluorescence imaging during robotic adrenalectomy. *J Surg Oncol*. 2016;114:153–156.

140. Hutteman M, van der Vorst JR, Mieog JS, et al. Near-infrared fluorescence imaging in patients undergoing pancreaticoduodenec-tomy. *Eur Surg Res*. 2011;47:90–97.

141. Bjurlin MA, McClintock TR, Stifelman MD. Near-infrared fluores-cence imaging with intraoperative administration of indocyanine green for robotic partial nephrectomy. *Curr Urol Rep*. 2015;16:20.

142. McClintock TR, Bjurlin MA, Wysock JS, et al. Can selective arterial clamping with fluorescence imaging preserve kidney function during robotic partial nephrectomy? *Urology*. 2014;84:327–332.

143. Bjurlin MA, Gan M, McClintock TR, et al. Near-infrared fluorescence imaging: emerging applications in robotic upper urinary tract surgery. *Eur Urol*. 2014;65:793–801.

144. Manny TB, Krane LS, Hemal AK. Indocyanine green cannot predict malignancy in partial nephrectomy: histopathologic correlation with fluorescence pattern in 100 patients. *J Endourol*. 2013;27:918–921.

145. Way LW, Stewart L, Gantert W, et al. Causes and prevention of laparoscopic bile duct injuries: analysis of 252 cases from a human factors and cognitive psychology perspective. *Ann Surg*. 2003;237:460–469.

146. Halawani HM, Tamim H, Khalifeh F, et al. Impact of intraoperative cholangiography on postoperative morbidity and readmission: analysis of the NSQIP database. *Surg Endosc*. 2016;30:5395–5403.

147. Speicher PJ, Goldsmith ZG, Nussbaum DP, et al. Ureteral stenting in laparoscopic colorectal surgery. *J Surg Res*. 2014;190:98–103.

148. Beraldo S, Neubeck K, Von Friderici E, Steinmuller L. The prophylactic use of a ureteral stent in laparoscopic colorectal surgery. *Scand J Surg*. 2013;102:87–89.

149. Halbert C, Altieri MS, Yang J, et al. Long-term outcomes of patients with common bile duct injury following laparoscopic cholecystec-tomy. *Surg Endosc*. 2016;30:4294–4299.

150. Halbert C, Pagkratis S, Yang J, et al. Beyond the learning curve: incidence of bile duct injuries following laparoscopic cholecystec-tomy normalize to open in the modern era. *Surg Endosc*. 2016;30: 2239–2243.

151. Tornqvist B, Stromberg C, Persson G, Nilsson M. Effect of intended intraoperative cholangiography and early detection of bile duct injury on survival after cholecystectomy: population based cohort study. *BMJ (Clinical Research ed)*. 2012;345:e6457.

152. Nuzzo G, Giuliante F, Giovannini I, et al. Bile duct injury during laparoscopic cholecystectomy: results of an Italian national survey on 56 591 cholecystectomies. *Arch Surg (Chicago, Ill: 1960)*. 2005;140:986–992.

153. Dip F, Roy M, Lo Menzo E, et al. Routine use of fluorescent incisionless cholangiography as a new imaging modality during laparoscopic cholecystectomy. *Surg Endosc*. 2015;29:1621–1626.

154. Dip FD, Asbun D, Rosales-Velderrain A, et al. Cost analysis and effectiveness comparing the routine use of intraoperative fluores-cent cholangiography with fluoroscopic cholangiogram in patients undergoing laparoscopic cholecystectomy. *Surg Endosc*. 2014;28: 1838–1843.

155. Larsen SS, Schulze S, Bisgaard T. Non-radiographic intraoperative fluorescent cholangiography is feasible. *Dan Med J*. 2014;61:A4891.

156. Prevot F, Rebibo L, Cosse C, et al. Effectiveness of intraoperative cholangiography using indocyanine green (versus contrast fluid) for the correct assessment of extrahepatic bile ducts during day-case laparoscopic cholecystectomy. *J Gastrointest Surg*. 2014;18: 1462–1468.

157. Spinoglio G, Priora F, Bianchi PP, et al. Real-time near-infrared (NIR) fluorescent cholangiography in single-site robotic cholecystectomy (SSRC): a single-institutional prospective study. *Surg Endosc*. 2013;27:2156–2162.

158. Schols RM, Bouvy ND, van Dam RM, et al. Combined vascular and biliary fluorescence imaging in laparoscopic cholecystectomy. *Surg Endosc*. 2013;27:4511–4517.

159. Schols RM, Bouvy ND, Masclee AA, et al. Fluorescence cholangiog-raphy during laparoscopic cholecystectomy: a feasibility study on early biliary tract delineation. *Surg Endosc*. 2013;27:1530–1536.

160. Buchs NC, Pugin F, Azagury DE, et al. Real-time near-infrared fluorescent cholangiography could shorten operative time during robotic single-site cholecystectomy. *Surg Endosc*. 2013;27: 3897–3901.

161. Kaneko J, Ishizawa T, Masuda K, et al. Indocyanine green reinjection technique for use in fluorescent angiography concomitant with cholangiography during laparoscopic cholecystectomy. *Surg Lapa-rosc Endosc Percutan Tech*. 2012;22:341–344.

162. Tagaya N, Shimoda M, Kato M, et al. Intraoperative exploration of biliary anatomy using fluorescence imaging of indocyanine green in

experimental and clinical cholecystectomies. *J Hepatobiliary Pancreat Sci*. 2010;17:595–600.

163. Ishizawa T, Bandai Y, Ijichi M, et al. Fluorescent cholangiography illuminating the biliary tree during laparoscopic cholecystectomy. *Br J Surg*. 2010;97:1369–1377.

164. Aoki T, Murakami M, Yasuda D, et al. Intraoperative fluorescent imaging using indocyanine green for liver mapping and cholangiography. *J Hepatobiliary Pancreat Sci*. 2010;17:590–594.

165. Ishizawa T, Tamura S, Masuda K, et al. Intraoperative fluorescent cholangiography using indocyanine green: a biliary road map for safe surgery. *J Am Coll Surg*. 2009;208:e1–e4.

166. Zarrinpar A, Dutson EP, Mobley C, et al. Intraoperative laparoscopic near-infrared fluorescence cholangiography to facilitate anatomical identification: when to give indocyanine green and how much. *Surg Innov*. 2016;23:360–365.

167. Kono Y, Ishizawa T, Tani K, et al. Techniques of fluorescence cholangiography during laparoscopic cholecystectomy for better delineation of the bile duct anatomy. *Medicine*. 2015;94:e1005.

168. Daskalaki D, Fernandes E, Wang X, et al. Indocyanine green (ICG) fluorescent cholangiography during robotic cholecystectomy: results of 184 consecutive cases in a single institution. *Surg Innov*. 2014;21: 615–621.

169. Ishizawa T, Kaneko J, Inoue Y, et al. Application of fluorescent cholangiography to single-incision laparoscopic cholecystectomy. *Surg Endos*. 2011;25:2631–2636.

170. Buchs NC, Hagen ME, Pugin F, et al. Intra-operative fluorescent cholangiography using indocyanin green during robotic single site cholecystectomy. *Int J Med Robot Comput Assist Surg*. 2012;8: 436–440.

171. Verbeek FP, Schaafsma BE, Tummers QR, et al. Optimization of near-infrared fluorescence cholangiography for open and laparoscopic surgery. *Surg Endosc*. 2014;28:1076–1082.

172. Mitsuhashi N, Kimura F, Shimizu H, et al. Usefulness of intra-operative fluorescence imaging to evaluate local anatomy in hepatobiliary surgery. *J Hepatobiliary Pancreat Sci*. 2008;15: 508–514.

173. Zroback C, Chow G, Meneghetti A, et al. Fluorescent cholangiography in laparoscopic cholecystectomy: the initial Canadian experience. *Am J Surg*. 2016;211:933–937.

174. Ankersmit M, van Dam DA, van Rijswijk AS, et al. Fluorescent imaging with indocyanine green during laparoscopic cholecystectomy in patients at increased risk of bile duct injury. *Surg Innov*. 2017;24:245–252.

175. Graves C, Ely S, Idowu O, et al. Direct gallbladder indocyanine green injection fluorescence cholangiography during laparoscopic cholecystectomy. *J Laparoendosc Adv Surg Tech A*. 2017;27:1069–1073.

176. Igami T, Nojiri M, Shinohara K, et al. Clinical value and pitfalls of fluorescent cholangiography during single-incision laparoscopic cholecystectomy. *Surg Today*. 2016;46:1443–1450.

177. van Dam DA, Ankersmit M, van de Ven P, et al. Comparing near-infrared imaging with indocyanine green to conventional imaging during laparoscopic cholecystectomy: a prospective crossover study. *J Laparoendosc Adv Surg Tech A*. 2015;25:486–492.

178. Osayi SN, Wendling MR, Drosdeck JM, et al. Near-infrared fluorescent cholangiography facilitates identification of biliary anatomy during laparoscopic cholecystectomy. *Surg Endosc*. 2015; 29:368–375.

179. Kawaguchi Y, Velayutham V, Fuks D, et al. Usefulness of indocyanine green-fluorescence imaging for visualization of the bile duct during laparoscopic liver resection. *J Am Coll Surg*. 2015;221:e113–1e117.

180. Boni L, David G, Mangano A, et al. Clinical applications of indocyanine green (ICG) enhanced fluorescence in laparoscopic surgery. *Surg Endosc*. 2015;29:2046–2055.

181. Dip F, Nguyen D, Montorfano L, et al. Accuracy of near infrared-guided surgery in morbidly obese subjects undergoing laparoscopic cholecystectomy. *Obes Surg*. 2016;26:525–530.

182. Liu YY, Liao CH, Diana M, et al. Near-infrared cholecystocholangiography with direct intragallbladder indocyanine green injection: preliminary clinical results. *Surgic Endosc*. 2018;32:1506–1514.

183. Boogerd LSF, Handgraaf HJM, Huurman VAL, et al. The best approach for laparoscopic fluorescence cholangiography: overview of the literature and optimization of dose and dosing time. *Surg Innov*. 2017;24:386–396.

184. Palaniappa NC, Telem DA, Ranasinghe NE, Divino CM. Incidence of iatrogenic ureteral injury after laparoscopic colectomy. *Arch Surg (Chicago, Il: 1960l)*. 2012;147:267–271.

185. Al-Taher M, van den Bos J, Schols RM, et al. Fluorescence ureteral visualization in human laparoscopic colorectal surgery using methylene blue. *J Laparoendosc Adv Surg Tech A*. 2016;26:870–875.

186. Lee Z, Simhan J, Parker DC, et al. Novel use of indocyanine green for intraoperative, real-time localization of ureteral stenosis during robot-assisted ureteroureterostomy. *Urology*. 2013;82:729–733.

187. Lee Z, Moore B, Giusto L, Eun DD. Use of indocyanine green during robot-assisted ureteral reconstructions. *Eur Urol*. 2015;67:291–298.

188. Morozov AO, Alyaev YG, Rapoport LM, et al. Near-infrared fluorescence with indocyanine green for diagnostics in urology: initial experience. *Urologia*. 2017;84:197–202.

189. Siddighi S, Yune JJ, Hardesty J. Indocyanine green for intra-operative localization of ureter. *Am J Obstet Gynecol*. 2014;211: 436e431–436e432.

190. Verbeek FP, van der Vorst JR, Schaafsma BE, et al. Intraoperative near infrared fluorescence guided identification of the ureters using low dose methylene blue: a first in human experience. *J Urol*. 2013;190:574–579.

191. Kassis ES, Kosinski AS, Ross P, Jr., et al. Predictors of anastomotic leak after esophagectomy: an analysis of the society of thoracic surgeons general thoracic database. *Ann Thorac Surg*. 2013;96: 1919–1926.

192. McDermott FD, Heeney A, Kelly ME, et al. Systematic review of preoperative, intraoperative and postoperative risk factors for colorectal anastomotic leaks. *Br J Surg*. 2015;102:462–479.

193. Karliczek A, Harlaar NJ, Zeebregts CJ, et al. Surgeons lack predictive accuracy for anastomotic leakage in gastrointestinal surgery. *Int J Colorectal Dis*. 2009;24:569–576.

194. Pacheco PE, Hill SM, Henriques SM, et al. The novel use of intraoperative laser-induced fluorescence of indocyanine green tissue angiography for evaluation of the gastric conduit in esophageal reconstructive surgery. *Am J Surg*. 2013;205:349–352. discussion 352-343.

195. Park YS, Lee CH, Park PJ, et al. Intraoperative contrast-enhanced sonographic portography combined with indigo carmine dye injection for anatomic liver resection in hepatocellular carcinoma: a new technique. *J Ultrasound Med*. 2014;33:1287–1291.

196. Shindoh J, Seyama Y, Umekita N. Three-dimensional staining of liver segments with an ultrasound contrast agent as an aid to anatomic liver resection. *J Am Coll Surg*. 2012;215:e5–e10.

197. Zehetner J, DeMeester SR, Alicuben ET, et al. Intraoperative assessment of perfusion of the gastric graft and correlation with anastomotic leaks after esophagectomy. *Ann Surg*. 2015;262:74–78.

198. Shimada Y, Okumura T, Nagata T, et al. Usefulness of blood supply visualization by indocyanine green fluorescence for reconstruction during esophagectomy. *Esophagus*. 2011;8:259–266.

199. Saito T, Yano M, Motoori M, et al. Subtotal gastrectomy for gastric tube cancer after esophagectomy: a safe procedure preserving the proximal part of gastric tube based on intraoperative ICG blood flow evaluation. *J Surg Oncol*. 2012;106:107–110.

200. Rino Y, Yukawa N, Sato T, et al. Visualization of blood supply route to the reconstructed stomach by indocyanine green fluorescence imaging during esophagectomy. *BMC Med Imaging*. 2014;14:18.

201. Murawa D, Hunerbein M, Spychala A, et al. Indocyanine green angiography for evaluation of gastric conduit perfusion during esophagectomy-first experience. *Acta Chir Belg*. 2012;112:275–280.

202. Kumagai Y, Ishiguro T, Haga N, et al. Hemodynamics of the reconstructed gastric tube during esophagectomy: assessment of outcomes with indocyanine green fluorescence. *World J Surg*. 2014;38:138–143.

203. Koyanagi K, Ozawa S, Oguma J, et al. Blood flow speed of the gastric conduit assessed by indocyanine green fluorescence: new predictive evaluation of anastomotic leakage after esophagectomy. *Medicine*. 2016;95:e4386.

204. Kamiya K, Unno N, Miyazaki S, et al. Quantitative assessment of the free jejunal graft perfusion. *J Surg Res*. 2015;194:394–399.

205. Campbell C, Reames MK, Robinson M, et al. Conduit vascular evaluation is associated with reduction in anastomotic leak after esophagectomy. *J Gastrointest Surg*. 2015;19:806–812.

206. Watanabe J, Ota M, Suwa Y, et al. Evaluation of the intestinal blood flow near the rectosigmoid junction using the indocyanine green fluorescence method in a colorectal cancer surgery. *Int J Colorectal Dis*. 2015;30:329–335.

207. Wada T, Kawada K, Takahashi R, et al. ICG fluorescence imaging for quantitative evaluation of colonic perfusion in laparoscopic colorectal surgery. *Surg Endos*. 2017;31:4184–4193.

208. Sherwinter DA, Gallagher J, Donkar T. Intra-operative transanal near infrared imaging of colorectal anastomotic perfusion: a feasibility study. *Colorectal Dis*. 2013;15:91–96.

209. Sherwinter DA. Transanal near-infrared imaging of colorectal anastomotic perfusion. *Surg Laparosc Endosc Percutan Tech*. 2012;22:433–436.

210. Ris F, Hompes R, Cunningham C, et al. Near-infrared (NIR) perfusion angiography in minimally invasive colorectal surgery. *Surg Endos*. 2014;28:2221–2226.

211. Protyniak B, Dinallo AM, Boyan WP, Jr., et al. Intraoperative indocyanine green fluorescence angiography-an objective evaluation of anastomotic perfusion in colorectal surgery. *Am Surg*. 2015;81:580–584.

212. Nishigori N, Koyama F, Nakagawa T, et al. Visualization of lymph/blood flow in laparoscopic colorectal cancer surgery by ICG fluorescence imaging (Lap-IGFI). *Ann Surg Oncol*. 2016;23:S266–S274.

213. Kudszus S, Roesel C, Schachtrupp A, Hoer JJ. Intraoperative laser fluorescence angiography in colorectal surgery: a noninvasive analysis to reduce the rate of anastomotic leakage. *Langenbeck's Arch Surg*. 2010;395:1025–1030.

214. Kin C, Vo H, Welton L, Welton M. Equivocal effect of intraoperative fluorescence angiography on colorectal anastomotic leaks. *Dis Colon Rectum*. 2015;58:582–587.

215. Kim JC, Lee JL, Yoon YS, et al. Utility of indocyanine-green fluorescent imaging during robot-assisted sphincter-saving surgery on rectal cancer patients. *Int J Med Robot Comput Assist Surg*. 2016;12:710–717.

216. Kawada K, Hasegawa S, Wada T, et al. Evaluation of intestinal perfusion by ICG fluorescence imaging in laparoscopic colorectal surgery with DST anastomosis. *Surg Endosc*. 2017;31:1061–1069.

217. Jafari MD, Wexner SD, Martz JE, et al. Perfusion assessment in laparoscopic left-sided/anterior resection (PILLAR II): a multi-institutional study. *J Am Coll Surg*. 2015;92:82–92.e81.

218. Jafari MD, Lee KH, Halabi WJ, et al. The use of indocyanine green fluorescence to assess anastomotic perfusion during robotic assisted laparoscopic rectal surgery. *Surg Endosc*. 2013;27:3003–3008.

219. Hellan M, Spinoglio G, Pigazzi A, Lagares-Garcia JA. The influence of fluorescence imaging on the location of bowel transection during robotic left-sided colorectal surgery. *Surg Endosc*. 2014;28:1695–1702.

220. Grone J, Koch D, Kreis ME. Impact of intraoperative microperfusion assessment with Pinpoint Perfusion Imaging on surgical management of laparoscopic low rectal and anorectal anastomoses. *Colorectal Dis*. 2015;17:22–28.

221. Foppa C, Denoya PI, Tarta C, Bergamaschi R. Indocyanine green fluorescent dye during bowel surgery: are the blood supply "guessing days" over? *Tech Coloproctol*. 2014;18:753–758.

222. Carus T, Dammer R. Laparoscop fluorescence angiography with indocyanine green to control the perfusion of gastrointestinal anastomoses intraoperatively. *Surg Technol Int*. 2012;22:27–32.

223. Boni L, Fingerhut A, Marzorati A, et al. Indocyanine green fluorescence angiography during laparoscopic low anterior resection: results of a case-matched study. *Surg Endosc*. 2017;31:1836–1840.

224. Boni L, David G, Dionigi G, et al. Indocyanine green-enhanced fluorescence to assess bowel perfusion during laparoscopic colorectal resection. *Surg Endosc*. 2016;30:2736–2742.

225. Bae SU, Baek SJ, Hur H, et al. Intraoperative near infrared fluorescence imaging in robotic low anterior resection: three case reports. *Yonsei Med J*. 2013;54:1066–1069.

226. Degett TH, Andersen HS, Gogenur I. Indocyanine green fluorescence angiography for intraoperative assessment of gastrointestinal anastomotic perfusion: a systematic review of clinical trials. *Langenbeck's Arch Surg*. 2016;401:767–775.

227. Uchiyama K, Ueno M, Ozawa S, et al. Combined intraoperative use of contrast-enhanced ultrasonography imaging using a sonazoid and fluorescence navigation system with indocyanine green during anatomical hepatectomy. *Langenbeck's Arch Surg*. 2011;396:1101–1107.

228. Inoue Y, Arita J, Sakamoto T, et al. Anatomical liver resections guided by 3-dimensional parenchymal staining using fusion indocyanine green fluorescence imaging. *Ann Surg*. 2015;262:105–111.

229. Kawaguchi Y, Nomura Y, Nagai M, et al. Liver transection using indocyanine green fluorescence imaging and hepatic vein clamping. *Br J Surg*. 2017;104:898–906.

230. Wagner OJ, Louie BE, Vallieres E, et al. Near-infrared fluorescence imaging can help identify the contralateral phrenic nerve during robotic thymectomy. *Ann Thorac Surg*. 2012;94:622–625.

231. Mangano MS, De Gobbi A, Beniamin F, et al. Robot-assisted nerve-sparing radical prostatectomy using near-infrared fluorescence technology and indocyanine green: initial experience. *Urologia*. 2018;85:29–31.

232. Chen SC, Wang MC, Wang WH, et al. Fluorescence-assisted visualization of facial nerve during mastoidectomy: a novel technique for preventing iatrogenic facial paralysis. *Auris Nasus Larynx*. 2015;42:113–118.

233. Whitney MA, Crisp JL, Nguyen LT, et al. Fluorescent peptides highlight peripheral nerves during surgery in mice. *Nat Biotechnol*. 2011;29:352–356.

234. Gibbs-Strauss SL, Nasr KA, Fish KM, et al. Nerve-highlighting fluorescent contrast agents for image-guided surgery. *Mol Imaging*. 2011;10:91–101.

235. Barth CW, Gibbs SL. Direct administration of nerve-specific contrast to improve nerve sparing radical prostatectomy. *Theranostics*. 2017;7:573–593.

236. Gray D, Kim E, Cotero V, et al. Compact fluorescence and white light imaging system for intraoperative visualization of nerves. *Proc SPIE Int Soc Opt Eng*. 2012;8207.

237. Park MH, Hyun H, Ashitate Y, et al. Prototype nerve-specific near-infrared fluorophores. *Theranostics*. 2014;4:823–833.

238. Verbeek FP, van der Vorst JR, Tummers QR, et al. Near-infrared fluorescence imaging of both colorectal cancer and ureters using a low-dose integrin targeted probe. *Ann Surg Oncol*. 2014;21:S528–S537.

239. Tummers QR, Boonstra MC, Frangioni JV, et al. Intraoperative near-infrared fluorescence imaging of a paraganglioma using methylene blue: a case report. *Int J Surg Case Report*. 2015;6c:150–153.

240. Winer JH, Choi HS, Gibbs-Strauss SL, et al. Intraoperative localization of insulinoma and normal pancreas using invisible near-infrared fluorescent light. *Ann Surg Oncol*. 2010;17:1094–1100.

241. Haque A, Faizi MS, Rather JA, Khan MS. Next generation NIR fluorophores for tumor imaging and fluorescence-guided surgery: a review. *Bioorg Med Chem*. 2017;25:2017–2034.

242. Guzzo TJ, Jiang J, Keating J, et al. Intraoperative molecular diagnostic imaging can identify renal cell carcinoma. *J Urol*. 2016;195:748–755.

243. van Dam GM, Themelis G, Crane LM, et al. Intraoperative tumor-specific fluorescence imaging in ovarian cancer by folate receptor-alpha targeting: first in-human results. *Nat Med*. 2011;17:1315–1319.

244. Shum CF, Bahler CD, Low PS, et al. Novel use of folate-targeted intraoperative fluorescence, otl38, in robot-assisted laparoscopic partial nephrectomy: report of the first three cases. *J Endourol Case Rep*. 2016;2:189–197.

245. Hoogstins CE, Tummers QR, Gaarenstroom KN, et al. A novel tumor-specific agent for intraoperative near-infrared fluorescence imaging: a translational study in healthy volunteers and patients with ovarian cancer. *Clin Cancer Res*. 2016;22:2929–2938.

246. Burggraaf J, Kamerling IM, Gordon PB, et al. Detection of colorectal polyps in humans using an intravenously administered fluorescent peptide targeted against c-Met. *Nat Med*. 2015;21:955–961.

247. Diana M, Halvax P, Dallemagne B, et al. Real-time navigation by fluorescence-based enhanced reality for precise estimation of future anastomotic site in digestive surgery. *Surg Endosc*. 2014;28:3108–3118.

248. Diana M, Dallemagne B, Chung H, et al. Probe-based confocal laser endomicroscopy and fluorescence-based enhanced reality for real-time assessment of intestinal microcirculation in a porcine model of sigmoid ischemia. *Surg Endosc*. 2014;28:3224–3233.

249. Diana M, Agnus V, Halvax P, et al. Intraoperative fluorescence-based enhanced reality laparoscopic real-time imaging to assess bowel perfusion at the anastomotic site in an experimental model. *Br J Surg*. 2015;102:e169–e176.

250. Diana M, Noll E, Diemunsch P, et al. Enhanced-reality video fluorescence: a real-time assessment of intestinal viability. *Ann Surg*. 2014;259:700–707.